Warm Temperature Promotes Shoot Regeneration in Arabidopsis thaliana

Alice Lambolez, Ayako Kawamura, Tatsuya Takahashi, Bart Rymen, Akira Iwase, David Favero, Momoko Ikeuchi, Takamasa Suzuki, Sandra S. Cortijo, Katja Jaeger, et al.

Warm Temperature Promotes Shoot Regeneration In *Arabidopsis thaliana*

Short title: Warm Temperature Promotes Shoot Regeneration

Corresponding author: K. Sugimoto, Cell Function Research Team, RIKEN Center for Sustainable Resource Science, 1-7-22 Suehiro-cho, Tsurumi, Yokohama, Kanagawa 230-0045, Japan, Telephone: +81-(0)45-503-9575, Fax: +81-(0)45-503-9591, Mail: keiko.sugimoto@riken.jp

Subject areas: growth and development, regulation of gene expression

Figures and tables:

- Black and white figures: 0,
- Color figures: 6,
- Tables: 0,
- Supplemental figures: 5,
- Supplemental tables: 2.

Warm Temperature Promotes Shoot Regeneration In *Arabidopsis thaliana*

Short title: Warm Temperature Promotes Shoot Regeneration

Authors: Alice Lambolez[1,2], Ayako Kawamura[1], Tatsuya Takahashi[1], Bart Rymen[1,3], Akira Iwase[1], David S. Favero[1], Momoko Ikeuchi[1,4], Takamasa Suzuki[5], Sandra Cortijo[6], Katja E. Jaeger[7], Philip A. Wigge[7] and Keiko Sugimoto[1,2*]

[1]RIKEN Center for Sustainable Resource Science, 1-7-22 Suehiro-cho, Tsurumi, Yokohama, Kanagawa 230-0045, Japan

[2]Department of Biological Sciences, Faculty of Science, The University of Tokyo, 7-3-1 Hongo, Bunkyō-ku, Tōkyō 113-8654, Japan

[3]Institut de Biologie Moléculaire des Plantes, 12 rue du Général Zimmer, 67084 Strasbourg, France

[4]Department of Biology, Faculty of Science, Niigata University, Ikarashi, Niigata 950-2181, Japan

[5]College of Bioscience and Biotechnology, Chubu University, 1200 Matsumoto-cho, Kasugai, Aichi, 487-8501, Japan

[6]UMR5004 Biochimie et Physiologie Moléculaire des Plantes, Université de Montpellier, CNRS, INRAE, Institut Agro, 2 place Pierre Viala, 34060, Montpellier, France

[7]Leibniz-Institut für Gemüse- und Zierpflanzenbau (IGZ) e.V., Theodor-Echtermeyer-Weg 1, 14979 Großbeeren,

Germany

*Corresponding author (Mail: keiko.sugimoto@riken.jp, Fax: +81-(0)45-503-9591)

Abstract

Many plants are able to regenerate upon cutting, and this process can be enhanced *in vitro* by incubating explants on hormone-supplemented media. While such protocols have been used for decades, little is known about the molecular details of how incubation conditions influence their efficiency. In this study, we find that warm temperature promotes both callus formation and shoot regeneration in *Arabidopsis thaliana*. We show that such an increase in shoot regenerative capacity at higher temperatures correlates with the enhanced expression of several regeneration-associated genes, such as *CUP-SHAPED COTYLEDON 1* (*CUC1*) encoding a transcription factor involved in shoot meristem formation and *YUCCAs* (*YUCs*) encoding auxin biosynthesis enzymes. ChIP-sequencing analyses further reveal that the histone variant H2A.Z is enriched on these loci at 17°C, while its occupancy is reduced by an increase in ambient temperature to 27°C. Moreover, we provide genetic evidence to demonstrate that H2A.Z acts as a repressor of *de novo* shoot organogenesis, since H2A.Z-depleted mutants display enhanced shoot regeneration. This study thus uncovers a new chromatin-based mechanism that influences hormone-induced regeneration and additionally highlights incubation temperature as a key parameter for optimizing *in vitro* tissue culture.

Keywords

temperature, regeneration, histone variant, H2A.Z, *Arabidopsis*

Introduction

Thanks to their extensive regenerative capacities, plants can repair tissues after an injury as well as regrow organs or even entire individuals from explants (Ikeuchi et al. 2016). These phenomena underlie many agricultural techniques that have been used for thousands of years, such as propagation by cutting (Howard 1971) and grafting (Melnyk 2016). However, not all plant species have equal regenerative capabilities, which impedes the large-scale culture and engineering of some recalcitrant crops, such as walnut (*Juglans regia*) or oak (*Quercus* spp.; Pijut et al. 2011). Barriers to regeneration can sometimes be overcome by controlling and directing the regeneration process *in vitro* through treatment of explants with different hormones (Skoog and Miller 1957; Che et al. 2007), a process hereinafter referred to as hormone-induced regeneration. This approach, widely used in both laboratory research and horticultural practice, has led to the establishment of new propagation techniques, such as *in vitro* embryo culture that has dramatically improved plantain (*Musa* spp.) and oil palm (*Elaeis guineensis*) yields (Vuylsteke and Swennen 1992; Weckx et al. 2019). Moreover, regeneration on hormone-supplemented medium is a key step in *Agrobacterium*-mediated transformation (Gelvin 2003), the main method used to generate transgenic plants. Thus, given its scientific and economic importance, establishing optimal conditions for hormone-induced regeneration is a crucial issue and requires a thorough understanding of the molecular mechanisms underlying this process.

Hormone-induced shoot regeneration is often performed using a two-step procedure, in which explants are first incubated on auxin-rich callus-inducing medium (CIM) and subsequently transferred to shoot-inducing medium (SIM) containing a high cytokinin/auxin ratio (Feldmann and Marks 1986). Incubation on CIM triggers

the formation of calli, unorganized masses of cells that undergo cellular reprogramming—defined here as the reconfiguration of cellular identity—through which they acquire regenerative competency (Ikeuchi et al. 2019). These calli exhibit several features that are also found in lateral root meristems (Sugimoto et al. 2010), including the auxin-induced and spatially organized expression of root meristem genes that appear to be necessary for the acquisition of cellular pluripotency (Kareem et al. 2015; 2018; Liu et al. 2018; Ikeuchi et al. 2019; Zhai and Xu 2021).

Subsequent shoot regeneration on SIM involves the conversion of these lateral root primordium-like structures into shoot-like structures. Auxin and cytokinin present in SIM permit the activation of *ENHANCER OF SHOOT REGENERATION 1* (*ESR1*) and its downstream paralog *ESR2*, which both contribute to the formation of shoot promeristems (Banno et al. 2001; Ikeda et al. 2006; Matsuo et al. 2011; Iwase et al. 2017). In particular, ESR2 directly activates *CUP-SHAPED COTYLEDON 1* (*CUC1*; Banno et al. 2001; Ikeda et al. 2006). CUC1 and its homolog CUC2 play a key role in shoot regeneration (Aida et al. 1997; Daimon et al. 2003) and are required for both development and maintenance of the shoot apical meristem (SAM; Aida et al. 1997; Gordon et al. 2007). In parallel, cytokinin contained in SIM promotes the expression of *WUSCHEL* (*WUS*), encoding a homeobox transcription factor required to initiate the formation of shoot progenitors (Gallois 2004; Gordon et al. 2007; Meng et al. 2017; Pernisova et al. 2018). Subsequent shoot meristem development is accompanied by the emergence of auxin- and cytokinin-response domains, which occupy mutually exclusive regions within the callus (Cheng et al. 2012). On one hand, SIM induces the expression of auxin biosynthesis enzymes *YUCCA 1* (*YUC1*) and *YUC4* and YUC-mediated auxin production in turn promotes SAM formation (Cheng et al. 2012). On the other hand, the domains producing cytokinin, a hormone that is required to stabilize WUS in regular SAM development (Snipes et al. 2018), are established at least in part by cytokinin biosynthesis enzymes of the ISOPENTENYLTRANSFERASE (IPT) family (Kakimoto 2001; Takei et al. 2001; Cheng et al. 2012).

While the molecular mechanisms underlying the developmental transitions that occur during regeneration are becoming increasingly clear, how environmental conditions impact these regeneration processes has not yet been thoroughly investigated (Ikeuchi et al. 2016). One of the major parameters affecting plant growth is ambient temperature, which influences numerous developmental processes such as hypocotyl and petiole growth (Gray et al. 1998; Koini et al. 2009) and timing of both flowering and silique dehiscence (Blázquez et al. 2003; Li et al. 2018). Such temperature-influenced plant development, termed thermomorphogenesis, is in part regulated at the chromatin level (Casal and Balasubramanian 2019). In particular, histone variant H2A.Z, encoded by *HISTONE H2A PROTEIN 8* (*HTA8*), *HTA9* and *HTA11* in *Arabidopsis thaliana* (March-Díaz and Reyes 2009), is evicted from nucleosomes when plants are exposed to warm temperature (Kumar and Wigge 2010; Cortijo et al. 2017). Accordingly, constitutively H2A.Z-depleted mutants phenocopy plants grown at higher temperatures, displaying for instance long hypocotyls and petioles (Kumar and Wigge 2010). H2A.Z-containing nucleosomes are predominantly found at transcription start sites (TSS) and on gene bodies (Kumar and Wigge 2010; Coleman-Derr and Zilberman 2012), where they are thought to prevent transcription (Thakar et al. 2010; Dai et al. 2017). This likely maintains genes in an off state that is poised for rapid activation in response to environmental cues, including temperature and light (Kumar and Wigge 2010; Coleman-Derr and Zilberman 2012; Cortijo et al. 2017; Willige et al. 2021). How H2A.Z is removed from nucleosomes in these contexts remains unclear, but recent evidence suggests that this depends on the activity of transcription factors, such as PHYTOCHROME-INTERACTING FACTOR 7 (PIF7) in response to light (Willige et al. 2021) or heat shock factors at the *HEAT SHOCK PROTEIN 70* (*HSP70*) locus in response to heat (Cortijo et al. 2017).

Although ambient temperature is briefly mentioned to modulate the efficiency of *in vitro* regeneration for several crops, such as tobacco (*Nicotiana tabacum*), sunflower (*Helianthus annuus*) or carrot (*Daucus carota*), in a now quite dated review (Haissig 1965), no molecular mechanisms explaining how temperature affects

hormone-induced regeneration have been reported so far. In this study, we show that warm temperature enhances both callus formation and subsequent shoot regeneration in *Arabidopsis thaliana*, and that the transcriptional events mediating this process correlate with temperature-dependent eviction of H2A.Z. Consistently, shoot regeneration is enhanced in double mutants for *HTA9* and *HTA11*, which resemble wild-type (WT) explants grown at a higher temperature. This study thus provides new insights into the temperature-dependent regulation of hormone-induced regeneration, and thereby lays a foundation for designing molecular approaches aimed at optimizing *in vitro* regeneration.

Results

Warm temperature accelerates hormone-induced callus formation and shoot regeneration

In order to first assess whether ambient temperature affects hormone-induced callus formation, we incubated hypocotyl explants from 7-day-old WT plants on CIM at 17°C, 22°C or 27°C, a temperature range that is considered not stressful for *Arabidopsis thaliana* (Kumar and Wigge 2010; Figures 1A and 1B). While a minor but significant decrease in fresh weight at 22°C or 27°C is observed after 4 days, likely due to water loss, this trend reverts later on. After 15 days on CIM, calli grown at 27°C are significantly heavier (2.5 times more on average) than those grown at 22°C, which are themselves significantly heavier than those grown at 17°C (3.2 times more on average). This positive effect of temperature on callus formation is even more pronounced after 25 days, as 27°C-grown calli are 4.6 times heavier than those grown at 22°C.

We next investigated how temperature affects hypocotyl explants transferred to SIM following a 4-day incubation on CIM, a stage at which calli grown at 17°C, 22°C or 27°C are morphologically indistinguishable from each other (Figure 1). A significant increase in shoots at warmer ambient temperature was observed from 11 days after transfer to SIM, when explants cultured at 27°C display 4.1 times more shoots than explants cultured at 22°C while none can be observed at 17°C (Figures 1C and 1D). Importantly, shoots are visible on explants cultured at 17°C 21 days after transfer on SIM, revealing that low temperature does not prevent shoot regeneration *per se*, but rather slows it down. In particular, at the point when leaves are just starting to appear at 17°C, 27°C-grown explants already present true leaves and start producing flower buds, indicating that the shoots regenerated at 27°C have already reached more mature developmental stages (Figure 1C). These results show that an increase in ambient temperature drastically accelerates hormone-induced regeneration in hypocotyl.

To check whether this behavior can be reproduced with other organs, we incubated root explants from 7-day-old WT plants for 21 days on CIM at either 17°C or 27°C (Supplemental Figures S1A and S1B). Similarly to what we had obtained with hypocotyls (Figures 1A and 1B), we observed an 18.1-fold increase in weight for explants grown at 27°C compared to those grown at 17°C (Supplemental Figures S1A and S1B). Likewise, root explants incubated for 4 days on CIM then 16 days on SIM at 27°C yield on average 37.1 shoots per explant whereas root explants incubated at 17°C do not show any shoots at this time point (Supplemental Figures S1C and S1D). These results show that the temperature-mediated acceleration of hormone-induced regeneration is not a hypocotyl-specific phenomenon.

As the positive influence of increased temperature on shoot regeneration could be due to its promotive effect on callus formation during CIM incubation, we tested whether ambient temperature affects shoot regeneration on SIM alone. We therefore incubated hypocotyl explants for 4 days on CIM at either 17°C or 27°C, and then for 11 days on SIM at 27°C or 17°C, respectively (Supplemental Figure S1E and S1F). We found that, at this time point, no shoot regeneration is observed on explants grown at 17°C on SIM, irrespective of the incubation

temperature on CIM (Supplemental Figure S1). We also observed that explants incubated continuously at 27°C display 1.3 times more shoots on average than explants grown on CIM at 17°C and then on SIM at 27°C (Supplemental Figure S1E and S1F). These results reveal that, while the temperature at which the incubation on CIM is performed does have an effect on explant growth, the temperature at which the incubation on SIM is performed appears to be the major factor contributing to the increase in shoot regeneration capacity, although this could also be due to the fact that the SIM step lasted longer than the CIM step in our experimental set-up.

Considering that wounding is essential for successful shoot regeneration upon external hormone application (Iwase et al. 2015), we tested if the positive effect of temperature seen during CIM and SIM incubation is a consequence of an enhanced wound response. We thus wounded 7-day-old WT hypocotyls and allowed them to regenerate without any hormone addition at 17°C, 22°C or 27°C (Supplemental Figure S2). We observed callus formation after wounding at all temperatures, and noticed a significant increase in the number of explants forming callus at warmer temperatures 6 days after cutting (1.4-fold increase at 22°C *versus* 17°C and 1.6-fold increase at 27°C *versus* 22°C), although these differences become non-significant at 21 days (Supplemental Figures S2A and S2B). Furthermore, we could not observe any clear correlation between ambient temperature and callus growth (Supplemental Figures S2A and S2C), suggesting that temperature may accelerate callus formation upon wounding, but this effect is likely too mild to explain the dramatic enhancement seen during hormone-induced regeneration.

Temperature affects the expression of a great number of regeneration and hormone-associated genes

In order to determine which genes are responsible for the increase in callus formation and shoot regeneration efficiency at higher temperatures, we performed RNA extraction followed by high-throughput sequencing (RNA-seq) on WT hypocotyl explants cultured at either 17°C or 27°C. Samples were harvested immediately after cut, right before transfer on SIM after 4 days on CIM, and after 4 days on SIM, *i.e.* before the emergence of the first shoots at 27°C (Figure 2, Supplemental Figure S3, Supplemental Table S1). By comparison with explants harvested immediately after cutting, we first found that 76.7% of genes up-regulated and 81.1% of genes down-regulated on CIM at 27°C show the same differential expression at 17°C (Supplemental Figure S3A). Likewise, 75.3% of genes up-regulated and 80.5% of genes down-regulated on SIM at 27°C show the same differential expression at 17°C. Moreover, we noticed that a significant number of genes up-regulated (47.3%) or down-regulated (50.9%) at 27°C compared to 17°C during CIM incubation are also up-regulated or down-regulated, respectively, at 27°C during SIM incubation (Supplemental Figure S3B). This suggests that non-stressful changes in ambient temperature tend to affect the amplitude of expression rather than the set of expressed genes, many of which are similarly regulated by exposure to CIM and SIM. In line with this hypothesis, genes up-regulated by increased temperature are significantly enriched (48.7%) with CIM- and SIM-induced genes (Figure 2A, Supplemental Table S1), whereas genes down-regulated by warm temperature are significantly enriched (45.7%) with CIM- and SIM-repressed genes (Supplemental Figure S3C, Supplemental Table S1). These data imply that combining an increase in temperature with the CIM/SIM protocol generates an additive effect that leads to enhanced regeneration.

To further investigate the genes that may play a role in enhancing regeneration at higher temperatures, we performed a Gene Ontology (GO) analysis on genes that are up-regulated at 27°C on CIM or SIM, and also induced by exposure to the same or both type of media (Figure 2B). As expected, we found a high enrichment for genes annotated with terms related to heat responses, such as “heat acclimation” (Figure 2B). More interestingly, we also found a high enrichment for genes annotated with terms related to shoot development, such as “secondary shoot formation”, and this GO category was represented even among genes induced by

warm temperature only during CIM incubation (Figure 2B). When performing a GO analysis on genes down-regulated by warm temperature and by CIM and/or SIM incubation (Supplemental Figure S3D), we found a high enrichment of stress-response genes, annotated with terms such as “response to water deprivation”, “response to wounding”, “response to salt stress” and “response to oomycetes”. This suggests that an increase in temperature may tilt the transcriptional balance between stress responses and growth pathways towards the latter.

We then investigated whether the expression of genes encoding transcription factors that are known to play a role in regeneration as well as histone modifiers and hormone-related factors that may participate in this process (Ikeuchi et al. 2017, 2019) is impacted by temperature (Supplemental Figures S3E and S3F). During CIM incubation, we found that an increase in temperature promotes the expression of genes implicated in cytokinin synthesis, such as *IPT1* and *LONELY GUY 3* (*LOG3*; Figure 2C, Supplemental Figure S3E). On SIM, warm temperature mostly induces genes coding for transcription factors involved in shoot development, such as *CUC1*, *CUC3*, *ESR2* and *WUS*, as well as genes involved in auxin synthesis, such as *YUC1* and *YUC4*, and auxin response, such as *SMALL AUXIN UPREGULATED 15* (*SAUR15*; Figure 2C, Supplemental Figure S3F). Notably, *YUC4* is also up-regulated by warm temperature during the CIM incubation step (Figure 2C). Altogether, these observations suggest that warm temperature affects regeneration in part by modifying the expression of transcription factor-coding genes as well as auxin- and cytokinin-related genes.

Warm temperature reduces H2A.Z occupancy on thermo-induced regeneration genes

Previous studies have shown that the alterations induced by temperature on plant development are linked with eviction of the histone variant H2A.Z (Kumar and Wigge 2010; Cortijo et al. 2017). It is thus possible that a similar mechanism improves hormone-induced regeneration efficiency at warmer temperatures. To test this hypothesis, we re-analyzed a chromatin immunoprecipitation followed by high-throughput sequencing (ChIP-seq) dataset from Cortijo et al. (2017), in which the genome-wide occupancy of HTA11 was assessed in whole WT seedlings grown at 17°C and then either shifted to 27°C or maintained at 17°C for 240 min (Figure 3, Supplemental Figure S4, Supplemental Table S2). We found that 6693 genes show reduced HTA11 enrichment at 27°C compared to 17°C, while 9541 genes gain HTA11 at 27°C (Figure 3A, Supplemental Figures S4A and S4B, Supplemental Table S2). This is in accordance with the results reported in Cortijo et al. (2017) and confirms that ambient temperature affects H2A.Z occupancy on many loci.

To assess whether regeneration genes are impacted by such changes in H2A.Z occupancy, we first compared the CIM- and/or SIM-induced genes up-regulated by temperature (Figure 2A) to genes showing modified HTA11 enrichment with an increase in temperature. We found that a significant proportion (26.3%) of these up-regulated genes lose HTA11 at 27°C, while another significant proportion (31.5%) gains HTA11 (Figure 3A). Surprisingly, performing the same comparison with CIM- and/or SIM-repressed genes down-regulated by temperature (Supplemental Figure S3C) returned similar results: 22.8% of down-regulated genes lose HTA11 after transfer to 27°C, while 40.9% gain HTA11 (Supplemental Figure S4B). As these results solely reflect the presence or absence of differential HTA11 enrichment at any location on the gene body, we next investigated the correlation between differential expression and HTA11 dynamics in a more quantitative and position-specific manner. To this end, we looked at the summed HTA11 enrichment on CIM/SIM-induced genes up-regulated at 27°C, CIM/SIM-repressed genes down-regulated at 27°C, as well as all other HTA11-marked genes (Figure 3B). We found that up-regulated and down-regulated genes display an overall higher enrichment of HTA11 compared to other HTA11-marked genes, which likely makes them more transcriptionally responsive to changes in H2A.Z occupancy (Figure 3B). Moreover, genes down-regulated at 27°C exhibit an overall higher HTA11 occupancy at

27°C than at 17°C, whereas HTA11 enrichment levels are lower at 27°C compared to 17°C on the gene body of up-regulated genes (Figure 3B). In particular, all 9 genes associated with regeneration that are strongly up-regulated at 27°C on CIM and/or SIM (Figure 2C) exhibit decreased HTA11 levels at this temperature, similar to *HSP70* which is induced both by temperature and loss of H2A.Z (Kumar and Wigge 2010; Figure 3C). This correlation between thermosensitive changes in HTA11 enrichment and differential gene expression suggests that loss of H2A.Z caused by an increase in ambient temperature could contribute to the induction of key genes during *in vitro* regeneration. Therefore, H2A.Z appears to mainly contribute to the regulation of hormone-induced regeneration by repressing gene expression, in accordance with previous results obtained in other developmental contexts (Thakar et al. 2010; Cortijo et al. 2017; Dai et al. 2017).

Loss of H2A.Z is sufficient to enhance hormone-induced regeneration

To further investigate this hypothesis, we assessed whether loss of H2A.Z causes enhanced hormone-induced callus formation and shoot regeneration, similar to incubation at warm temperature. We thus performed *in vitro* regeneration procedures using explants from WT and two double mutants for the H2A.Z proteins, namely *hta9-1;hta11-1* and *hta9-1;hta11-2*. We did not use *hta8;hta9;hta11* triple mutants, which completely lack H2A.Z, as they show very strong developmental defects (Coleman-Derr and Zilberman 2012).

We first investigated callus formation in these double mutants by incubating hypocotyl explants for 17 days at 22°C on CIM (Supplemental Figures S5A and S5B) and observed no significant difference with WT explants. Therefore, we cannot conclude from this experiment that H2A.Z eviction contributes to the enhancement of callus formation by warm temperature.

In contrast, results were more consistent with our expectations when looking at shoot regeneration in these mutant explants after 4 days on CIM and then 11, 16 or 29 days on SIM at either 17°C, 22°C or 27°C (Figure 4). We first noticed that only explants incubated at 27°C present shoots 11 days after transfer on SIM, when explants incubated at lower temperatures are still devoid of them (Figures 4A and 4B). Similarly, 16 days after transfer on SIM, shoots are visible on explants incubated at 22°C or 27°C but remain absent from explants incubated at 17°C (Figures 4C and 4D). As this applies to both WT and *hta9;hta11* explants, this suggests that loss of H2A.Z at warmer temperatures poorly explains the dramatic acceleration of shoot regeneration observed in these conditions. We then examined the enhancement of shoot regeneration in *hta9;hta11* explants compared to WT explants in function of the incubation temperature, using time points at which WT explants showed a similar regenerative progress for each condition (> 0 and < 50 shoots per explant, *i.e.* 11 days after transfer on SIM at 27°C, 16 days after transfer on SIM at 22°C and 29 days after transfer on SIM at 17°C; Figures 4B, 4D, 4F). At 17°C, *hta9-1;hta11-1* explants produce 2.5 times and *hta9-1;hta11-2* explants 2.1 times more shoots on average than WT explants (Figure 4F) whereas at 22°C, *hta9-1;hta11-1* explants produce 1.9 times and *hta9-1;hta11-2* explants 2.1 times more shoots on average (Figure 4D). Following the same trend, at 27°C *hta9-1;hta11-1* explants produce 1.6 times more shoots on average than WT explants while no significant difference is detected between WT and *hta9-1;hta11-2* explants (Figure 4B). The positive effect of the *hta9;hta11* double mutation on *de novo* shoot organogenesis thus appears to be reduced at 27°C compared to 17°C, indicating that loss of H2A.Z is sufficient to enhance shoot regeneration on SIM and that this effect largely contributes to the increased shoot production observed at warmer temperatures (Figures 1C and 1D).

Increased CUC1 *expression contributes to enhanced shoot regeneration at warmer temperatures*

We ultimately sought to check whether up-regulation of the regeneration genes putatively affected by H2A.Z

eviction (Figure 2C) is indeed responsible for the enhancement of callus formation and shoot regeneration at warm temperature. In particular, among genes for which up-regulation at 27°C correlates with H2A.Z loss (Figures 2C and 3C), we focused our attention on *CUC1*, since its overexpression is known to enhance shoot regeneration at 22°C (Daimon et al. 2003). To test if a lack of H2A.Z is sufficient to induce *CUC1* expression, we performed a reverse transcription followed by quantitative polymerase chain reaction (RT-qPCR) assay on total RNA extracted from WT and *hta9-1;hta11-1* hypocotyl explants which were incubated on CIM for 4 days then on SIM for 4 days at either 17°C or 27°C (Figure 5A). In accordance with our hypothesis, we observed increased *CUC1* expression in *hta9-1;hta11-1* at all assessed time points when explants were incubated at 17°C (Figure 5A). While this is also true at 27°C for explants incubated on CIM, the difference in the amount of *CUC1* transcripts between *hta9-1;hta11-1* and WT becomes non-significant when these explants are transferred to SIM (Figure 5A). These results suggest that, in terms of *CUC1* expression, *hta9-1;hta11-1* is less sensitive than WT to an increase in temperature during hormone-induced shoot regeneration. Moreover, using expression array data published in Takeda et al. (2011), where the authors assayed the transcriptional landscape of 5-day-old cotyledons from a *35S::CUC1* overexpressor, we found a significant overlap between genes up-regulated in *35S::CUC1* and those up-regulated at 27°C compared to 17°C (Figure 5B), implying that the CUC1-mediated transcriptional pathway is enhanced at 27°C.

We therefore investigated the callus formation and shoot regeneration abilities of *cuc1-13* hypocotyls at 17°C and 27°C (Supplemental Figures S5C and S5D, Figures 5C and 5D). We found that *cuc1-13* calli grown on CIM for 15 days weigh more than WT calli at both 17°C and 27°C (Supplemental Figures S5C and S5D). However, different results were observed in explants incubated on CIM for 4 days and then on SIM for 11 days (Figures 5C and 5D). At 17°C, where *CUC1* is only slightly induced on SIM (Figure 2C), no shoots were observed in WT nor *cuc1-13* explants. At 27°C, where *CUC1* is dramatically induced on SIM (Figure 2C), explants from both genotypes exhibit shoot formation, but *cuc1-13* explants produce substantially fewer shoots (6.1 times less; Figures 5C and 5D). Altogether, these observations strongly suggest that up-regulation of *CUC1* at 27°C contributes to the thermosensitive enhancement of shoot regeneration.

YUC activity is required for the enhancement of shoot regeneration at warmer temperatures

Our selection of warmth-induced regeneration genes that concomitantly lose H2A.Z (Figures 2C and 3C) additionally features an auxin-responsive factor, *SAUR15*, as well as two genes coding for auxin biosynthesis enzymes, *YUC1* and *YUC4*. Members of the YUC family play a role in thermomorphogenesis (Sun et al. 2012; Gyula et al. 2018) and higher auxin concentrations are known to enhance shoot regeneration to a certain extent (Skoog and Miller 1957; Ikeuchi et al. 2019). Moreover, *YUC1* and *YUC4* have previously been shown to be induced on SIM and double mutants for these genes exhibit drastically reduced shoot regeneration frequency (Cheng et al. 2012). Using the same reasoning and the same RT-qPCR assay described previously for *CUC1* (Figure 5A), we evaluated the expression of *YUC1* and *YUC4* in *hta9-1;hta11-1* during shoot regeneration at 17°C and 27°C (Figure 6A). On one hand, we found that the *hta9-1;hta11-1* mutation does not affect *YUC1* expression on CIM or SIM at 17°C and leads to diverging results at 27°C, with a 75.8% increase in *YUC1* transcripts on CIM and a 37.8% decrease on SIM (Figure 6A). It thus appears that loss of H2A.Z is not a promoting event for *YUC1* expression. On the other hand, we observed that *YUC4* expression is increased in *hta9-1;hta11-1* compared to WT after 4 days on SIM at 17°C (21.4% more), but not at 27°C (Figure 6A). Consequently, like for *CUC1* (Figure 5A), H2A.Z depletion at 27°C seems to promote *YUC4* transcription in these conditions. Furthermore, we found a very strong overlap when comparing genes up-regulated at 27°C with genes up-regulated by a 3-day application of 4.5 µM exogenous auxin (NAA) in 15-day-old rosette leaves

(Figure 6B), which were obtained by re-analyzing a RNA-seq dataset published by Zia et al. (2019). Increased auxin biosynthesis due to the up-regulation of *YUC1* and/or *YUC4* may therefore also explain the enhancement of callus formation and shoot regeneration at 27°C and in *h2a.z* mutants.

To test this hypothesis, we first incubated WT hypocotyl explants on CIM supplemented with or without 10 µM 5-(4- chlorophenyl)-4H-1,2,4-triazole-3-thiol (yucasin), a YUC inhibitor (Nishimura et al. 2014), for 17 days at 17°C or at 27°C (Supplemental Figures S5E and S5F). At 17°C, explants show mildly increased callus formation upon exposure to yucasin, although the significance of this increase weakens at 27°C, strongly suggesting that elevated YUC activity does not contribute to increased callus formation on CIM at higher temperatures. We next incubated WT explants for 4 days on CIM supplemented with or without 10 µM yucasin and then for 13 days on SIM supplemented with or without 10 µM yucasin, at either 17°C or 27°C (Figures 6C and 6D). As expected at 17°C, where *YUC4* is only mildly induced on CIM and SIM (Figure 2C), we observed no difference between explants submitted to different treatments (Figures 6C and 6D). At 27°C, where *YUC4* is highly induced on CIM/SIM (Figure 2C), the number of shoots produced per explants decreases as the time of exposure to yucasin increases; in particular, explants grown at 27°C and exposed to yucasin during SIM incubation largely resemble those grown at 17°C (Figures 6C and 6D). These observations strongly suggest that increased YUC activity is partially responsible for enhancing shoot regeneration at 27°C. Interestingly, while YUC activity during CIM incubation does not seem necessary for callus formation *per se*, it does appear to be required on CIM for proper shoot regeneration later on, as inhibition of auxin biosynthesis on this medium alone leads to significantly reduced shoot regeneration in explants incubated at 27°C (3.7 times less; Figure 6D). However, we cannot exclude that this effect results from yucasin being carried over in the explants during the transfer from CIM to SIM. Nevertheless, these results together support the idea that temperature enhances shoot regeneration *via* the up-regulation of genes coding for transcription factors such as CUC1 as well as auxin biosynthesis enzymes such as YUC4.

Discussion

Warm ambient temperature promotes hormone-induced callus formation and shoot regeneration

In this study we uncovered a new parameter that influences the efficiency of hormone-induced regeneration in *Arabidopsis thaliana*. Our CIM/SIM assays demonstrate that an increase in ambient temperature improves both callus formation on CIM and shoot regeneration on SIM (Figure 1). Likely because the temperature range used in this study is not very stressful for *Arabidopsis thaliana* (Kumar and Wigge 2010), warm temperature appears to primarily amplify changes in the transcription of genes that are already affected by the hormones present in CIM and SIM (Supplemental Figure S3A).

Our observations suggested that warm temperature enhances shoot regeneration by affecting multiple pathways ranging from transcriptional regulation of shoot meristem formation to auxin biosynthesis (Figures 5 and 6). These results could reflect the global enhancement of plant growth at warm temperatures. In particular, we predict that the transcription factor CUC1 plays an important role in the response to temperature since its expression is strongly enhanced at 27°C (Figures 2C and 5A) and a previous study showed that *CUC1* overexpression in *35S::CUC1* explants promotes shoot regeneration at 22°C (Daimon et al. 2003). While no clear connections have previously been made between *CUC1* and thermosensitive development, its homologs *CUC2* and *CUC3*, which are also up-regulated at 27°C on SIM (Supplemental Figure S3F), are known to define leaf morphogenesis (Nikovics et al. 2006; Hasson et al. 2011), a process which is affected by ambient temperature in various species (Royer 2012; Nakayama et al. 2014; McKee et al. 2019). It is thus possible that

members of the CUC family act as downstream effectors of thermo-sensory responses in contexts other than regeneration.

Our data further showed that YUC-mediated auxin biosynthesis is a key downstream pathway important for the temperature response. We found that two members of the *YUC* family, *YUC1* and *YUC4*, are up-regulated during CIM and/or SIM incubation at 27°C (Figure 2C) and that application of a YUC inhibitor decreases the enhancement of shoot regeneration by higher temperatures (Figures 6C and 6D). Previous studies have shown that warm temperatures increase auxin levels by stimulating the expression of *YUC4* and *YUC8* (Gray et al. 1998; Sun et al. 2012). Moreover, mutants deficient in auxin synthesis display defective hypocotyl elongation and leaf hyponasty in response to warm temperature (Gray et al. 1998; Sun et al. 2012). These observations, together with our results, strongly suggest that responses to warm temperature heavily rely on elevated auxin levels promoted by an increase in its biosynthesis during regular development and *de novo* shoot organogenesis. As demonstrated for *CUC1* (Daimon et al. 2003), it will be interesting to test whether *YUC* overexpression alone is sufficient to mimic increased shoot regeneration at warm temperatures. Intriguingly, increased *YUC* expression does not appear to account for improved callus formation on CIM, as this process is not affected by chemical inhibition of YUCs (Supplemental Figures S5E and S5F). Given that none of the pathways investigated in this study explain how an increase in ambient temperature enhances hormone-induced callus formation, further research is needed to understand the molecular basis of this phenomenon.

It should also be noted that multiple cellular pathways that underlie hormone-induced regeneration, such as cell proliferation and fate change, appear to be enhanced at 27°C compared to lower temperatures (Figure 1). This leads us to predict that the developmental effects of warm temperature described in this study may be restricted to or strongly exaggerated in the context of *in vitro* culture on regenerative media. In line with this idea, we additionally found that warm temperature poorly influences wound-induced callus formation at the cut site in hypocotyls (Supplemental Figure S2). Accordingly, our GO analysis revealed that many wound response genes are down-regulated by warm temperature (Supplemental Figure S3D). However, this result could simply be due to the timepoints at which our RNA-seq samples were harvested (4 days and 8 days after cutting) as wound responses are activated quite rapidly (within 24 hours after cutting; Ikeuchi et al. 2017; Rymen et al. 2019). Despite this caveat, these observations bring additional evidence that the processes of hormone- and wound-induced callus formation are regulated differently. This is consistent with previous results showing divergent roles for epigenetic modifiers, such as HISTONE ACETYLTRANSFERASE OF THE GNAT FAMILY 1 (HAG1), in the regulation of CIM-induced callus formation *versus* wound-induced callus formation (Kim et al. 2018; Rymen et al. 2019).

An increase in temperature relieves the H2A.Z-mediated repression of shoot regeneration

Our study brings new evidence suggesting that the influence of warm temperature on *de novo* shoot organogenesis is regulated by H2A.Z. Kumar and Wigge (2010) first enunciated the model in which an increase in temperature induces H2A.Z eviction and thereby modifies the expression of numerous thermosensitive genes. Our results expand this model to the context of hormone-induced regeneration, and confirm that H2A.Z is a dynamic mark conferring transcriptional sensitivity to the environment in plants, as proposed by Coleman-Derr and Zilberman (2012). It should be noted that some studies have proposed a dual regulatory role for H2A.Z when located close to the TSS, where it is suggested to act both as transcriptional activator and a transcriptional repressor depending on the context (Zilberman et al. 2008; Coleman-Derr and Zilberman 2012; Sura et al. 2017; Gómez-Zambrano et al. 2019). However, in our study, elevated H2A.Z occupancy close to the TSS was mainly associated with repressive effects (Figure 3). Importantly, by choosing to reanalyze a previously published ChIP-

seq dataset that examines early responses to warm temperatures (Cortijo et al. 2017), we did not assess H2A.Z occupancy at the same time points at which we evaluated gene expression or regeneration phenotypes. Further work is therefore needed to determine whether the H2A.Z landscape remain unchanged throughout CIM/SIM incubation at warm or cool temperature. Nevertheless, our RT-qPCR assays (Figures 5A and 6A) clearly demonstrate that, like in an *hta9;hta11* mutant where H2A.Z levels are constitutively reduced, exposure to 27°C promotes *CUC1* or *YUC4* transcription in WT explants after 4 days on SIM, suggesting that H2A.Z occupancy remains low during prolonged incubation at warm temperatures. In addition, as we detected the strongest differential expression at this time point, *i.e.* when *CUC1* or *YUC4* are the most transcribed (Figure 2C), we hypothesize that a reduction in H2A.Z levels alone may not be sufficient to induce the expression of target regeneration genes, but rather creates a chromatin environment that facilitates their up-regulation by hormone-responsive factors upon exposure to SIM. Moreover, our phenotyping results using yucasin (Figures 6C and 6D) are consistent with those obtained by Lee and Seo (2017), who showed that application of this inhibitor to mutants for *ARP6*, encoding a subunit of the SWR1 complex that catalyzes the deposition of H2A.Z (March-Díaz and Reyes 2009), rescues their elongated hypocotyl phenotype caused by *YUC9* overexpression.

Purified *Arabidopsis* H2A.Z-containing nucleosomes show no direct reduction of DNA-histone octamer association upon changes in ambient temperature *in vitro* (Cortijo et al. 2017), revealing the existence of a sensory mechanism responsible for detecting temperature fluctuations and translating it to H2A.Z occupancy *in vivo*. Recent studies have unveiled the role of the INO80 chromatin remodeling complex (Zander et al. 2019; Willige et al. 2021; Xue et al. 2021) and/or of specific transcription factors for H2A.Z eviction upon environmental cues, such as PIF7 in the response to changes in light quality (Willige et al. 2021), PIF4 during thermomorphogenesis (Xue et al. 2021) or heat shock factors for *HSP70* induction at warm temperature (Cortijo et al. 2017). Whether the temperature-mediated relief of H2A.Z repression on shoot regeneration genes depends on the function of such factors should therefore be addressed in future studies.

Although we observed significantly enhanced shoot regeneration in mutants for the *HTA* genes at 22°C, these mutants do not completely phenocopy explants cultured at 27°C (Figures 1 and 4). This could be due to none of the tested mutants being null for H2A.Z, but may also suggest that our H2A.Z-based model is not the only mechanism by which temperature affects hormone-induced regeneration. H2A.Z eviction may mainly contribute to the temperature response by increasing chromatin accessibility, but likely does not explain all other effects induced by warmth, such as the recruitment of thermosensitive transcription factors to their target promoters. In addition, other epigenetic marks may also contribute to the enhancement of regeneration by temperature. For instance, repressive histone H3 lysine 27 trimethylation (H3K27me3) has been associated with the regulation of thermosensitive processes such as flowering (Noh et al. 2004; Zheng et al. 2019), and seedlings unable to catalyze H3K27me3 spontaneously form callus structures (Bouyer et al. 2011). Moreover, H3K27me3 co-localizes with H2A.Z (Carter et al. 2018), for example on the *YUC4* loci (Lu et al. 2019), and is hypothesized to regulate common transcriptional networks (Carter et al. 2018). Another histone modification mark, histone H3 lysine 9 acetylation (H3K9ac), has been more clearly linked to the regulation of thermomorphogenesis. Specifically, warm temperature promotes POWERDRESS (PWR) to recruit HISTONE DEACETYLASE 9 (HDA9) to the *YUC8* locus and thereby maintains low levels of H3K9ac at its +1 nucleosome (Tasset et al. 2018). This was reported to be critical for proper H2A.Z eviction by warm temperature (van der Woude et al. 2019) and thus makes it a candidate mechanism worth investigating.

Given that our results were all obtained using *Arabidopsis thaliana* ecotype Columbia, whether exposure to warm temperature and/or loss of H2A.Z similarly enhances hormone-induced regeneration in other ecotypes or plant species, notably those that are more recalcitrant to regeneration (Benson 2000; Motte et al. 2014; Lardon et al. 2020), would be an interesting question to address in future research. Previous studies showed that

various *Arabidopsis* ecotypes display diverse degrees of regeneration efficiency (Motte et al. 2014; Lardon et al. 2020), which leads us to predict that some respond to temperature cues in a similar manner. Moreover, as temperature impacts the development and yield of numerous crop species such as tomato (*Lycopersicon esculentum*; Adams et al. 2001), wheat (*Triticum* spp.; Wang et al. 2017), corn (*Zea mays*), soybean (*Glycine max*) and cotton (*Gossypium* spp.; Schlenker and Roberts 2009), warm temperatures may likewise promote shoot regeneration in these species. In particular, H2A.Z is one of the most conserved histone variants among eukaryotes (Thatcher and Gorovsky 1994) and also regulates responses to temperature in *Brachypodium distachyon* (Boden et al. 2013). H2A.Z may thus have an analogous repressor role in the regeneration of other plants and this possibility as well as its potential downstream applications should be thoroughly investigated.

Materials and Methods

Plant materials and growth conditions

All *Arabidopsis thaliana* plants used in this study are ecotype Columbia (Col-0), from the following accessions: SALK_054814 crossed with SALK_017235 (*hta9-1;hta11-1*), SALK_054814 crossed with SALK_031471 (*hta9-1;hta11-2*) and SALK_006496 (*cuc1-13*). These alleles were previously described in March-Díaz et al. (2007; *hta9-1;hta11-1*), Xu et al. (2017; *hta9-1;hta11-2*) and Hibara et al. (2006; *cuc1-13*). Plants were grown on nylon mesh placed on Murashige-Skoog (MS) medium containing 1% sucrose and 0.6% (w/v) gelzan. Plates were placed vertically at 22°C in SANYO MLR-352 (Panasonic®) growth chambers with an unmonitored humidity varying from 24% to 57%, and kept in the dark for 7 days to induce hypocotyl elongation.

Callus formation and shoot regeneration

For hormone-induced callus formation, 7-day-old etiolated seedlings were dissected with a razor blade to generate hypocotyl explants, which were taken from the region spanning ~3 mm above the root/hypocotyl junction and ~5 mm below the hypocotyl/shoot junction, or root explants, which were taken from the region spanning ~4 to ~14 mm below the root/hypocotyl junction. Explants were incubated in the growth chambers described above under constant fluorescent white light (~50 $\mu mol.m^{-2}.s^{-1}$) at the specified temperatures and for the indicated number of days on CIM, *i.e.* MS medium supplemented with Gamborg's B5 vitamin, 20 $g.L^{-1}$ glucose, 0.5 $g.L^{-1}$ 2-(N-morpholino)ethane-sulfonic acid (MES), 7.5 $g.L^{-1}$ Gellan gum, 0.1 $mg.L^{-1}$ kinetin and 0.5 $mg.L^{-1}$ 2,4-dichlorophenoxyacetic acid (2,4 D; Valvekens et al. 1988). To induce shoot regeneration, explants incubated for 4 days on CIM were transferred to SIM, *i.e.* MS medium supplemented with Gamborg's B5 vitamin, 20 $g.L^{-1}$ glucose, 0.5 $g.L^{-1}$ MES, 2.5 $g.L^{-1}$ Gellan gum, 0.5 $mg.L^{-1}$ N6-(2-isopentenyl)adenine (2-iP) and 0.15 $mg.L^{-1}$ indole-3-acetic acid (IAA; Valvekens et al. 1988). The explants were then incubated in the same conditions as for CIM, at the specified temperatures and for the indicated number of days. To assess the importance of auxin biosynthesis in the context of hormone-induced callus formation and shoot regeneration, CIM and/or SIM were supplemented with 10 µM yucasin (CAS No. 26028-65-9, Wako®, FUJIFILM®; Nishimura et al. 2014), and dimethyl sulfoxide (DMSO) was used as control. To measure fresh weight, explants were dabbed on a Kimwipe® paper tissue to remove media and weighed five at a time using an XS104 balance (Mettler Toledo®). Weight values were then normalized based on the summed initial lengths of the corresponding explants. Shoot regeneration efficiency was quantified as the number of shoots displayed by each explant.

For wound-induced callus formation, 7-day-old seedlings were cut with a razor blade ~7 mm above the

root/hypocotyl junction. For each seedling, the apical part was removed and the remaining portion was left on the same plate of MS medium and incubated vertically, in the dark and at the specified temperature for the indicated number of days. Callus formation was quantified by counting, per plate, the number of explants showing at least 2 newly formed cells at the wound-site when observed using a dissecting microscope. To calculate callus area projections, calli were photographed using DIC microscopy with an Olympus® BX51 microscope and their edges were manually traced on the resulting pictures using a graphic tablet (XP-PEN® Artist 22E Pro). The filling areas were measured with ImageJ (version 1.52p).

All assays were replicated on at least 3 different plates per genotype and/or condition.

RNA extraction, sequencing and data analysis

Total RNA was isolated from hypocotyl explants incubated in the specified conditions in triplicates. For each replicate, ~100 hypocotyls were harvested and frozen with liquid nitrogen. The samples were then ground using zirconia ceramic beads in a TissueLyser™ (QIAGEN ®) mixer mill. RNA was extracted using the RNeasy® Plant Mini kit (QIAGEN®) following the manufacturer's instructions. Libraries for sequencing were prepared using the KAPA Stranded mRNA-seq Kit™ (Kapa Biosystems®, Roche®) with a mix of FastGene™ (Nippon Genetics®) and NEBNext® (New England Biolabs®) adapters, and sequencing was performed on an Illumina® NextSeq™ 500 platform in single-end.

Raw sequencing files were processed on a virtual machine running on Ubuntu (version 18.04.1). Sequencing quality was first checked using FastQC (version 0.11.7; Andrews 2010). Reads were then mapped to the TAIR10 *Arabidopsis thaliana* genome using Bowtie2 (version 2.3.4.3; Langmead and Salzberg 2012) with the "`--no-1mm-upfront`" option, and further processed using the samtools (version 1.9; Li et al. 2009) functions `view`, `sort`, `rmdup` and `index`. The read mapping rate was > 55% for all RNA-seq samples. Read counts per gene were determined using the `multicov` function from bedtools (version 2.26.0; Quinlan and Hall 2010). Differential expression analyses were performed on R (version 3.4.4; R Core Team 2021) with the "edgeR" package (version 3.22.5; Robinson et al. 2009; McCarthy et al. 2012). Genes with an absolute fold change > 1.5 and a false discovery rate (edgeR) < 0.001 were considered differentially expressed. Venn diagrams were drawn using the R package "Vennerable" (version 3.0; Swinton 2013) and line plots and heatmaps were plotted using the R packages "gplots" (version 3.0.1; Warnes et al. 2020) and "ggplot2" (version 3.1.0; Wickham 2016). Figures were assembled in R with packages "grid" (version 3.5.1; R Core Team 2021), "gridExtra" (version 2.3; Auguie 2017), "cowplot" (version 0.9.3; Wilke 2020) and "ggplotify" (version 0.0.3; Yu 2020), and further refined in Inkscape (version 0.92.3).

The same *in silico* analyses were performed on the raw files from the RNA-seq dataset in 15-day-old rosettes exposed to an external application of auxin, which was previously published in Zia et al. (2019).

Gene Ontology (GO) enrichment analysis

GO analyses were performed on R (version 3.4.4; R Core Team 2021) using the "biomaRt" (version 2.38.0; Durinck et al. 2005, 2009), "GO.db" (version 3.7.0; Carlson 2020) and "topGO" (version 2.34.0; Alexa and Rahnenfuhrer 2020) packages. For each gene category, the 10 most enriched terms were selected (Fisher's exact test). Figures were drawn using the R packages "gplots" (version 3.0.1; Warnes et al. 2020) and "ggplot2" (version 3.1.0; Wickham 2016).

ChIP-seq data analysis

The dataset from the HTA11 ChIP-seq performed at 17°C and 27°C in WT whole seedlings was previously published in Cortijo et al. (2017). Raw sequencing files were processed on a virtual machine running on Ubuntu (version 18.04.1). Sequencing quality was first checked using FastQC (version 0.11.7; Andrews 2010), then reads were mapped to the TAIR10 *Arabidopsis thaliana* genome using Bowtie2 (version 2.3.4.3; Langmead and Salzberg 2012) with the "`--no-1mm-upfront`" option, and further processed using the samtools (version 1.9; Li et al. 2009) functions `view`, `sort`, `rmdup` and `index`. The read mapping rate was > 62% for all samples. Peak-calling was performed using SICER2 (version 1.1; Xu et al. 2014) without a control and with the following parameters: window size 200 bp; fragment size 150 bp; effective genome fraction 0.74; FDR cutoff 0.01; gap size minimum 600 bp; e-value 1000. Peaks obtained from at least 2 replicates were extracted and merged using the bedtools (version 2.26.0; Quinlan and Hall 2010) functions `intersect` and `merge`. These peaks were then mapped to TAIR10 genes using bedtools `intersect`. In total, 13,628 peaks intersecting with 21,378 genes were detected at 17°C and 15,542 peaks intersecting with 22,756 genes were detected at 27°C. The HTA11 enrichment of each gene was calculated as the mean coverage of all its intersecting peaks. Differentially marked genes were defined as genes with a ratio "enrichment at 27°C / enrichment at 17°C" > 1.2 or < 0.8. Coverage BigWig files were produced using the deepTools (version 3.2.1; Ramírez et al. 2014) function `bamCoverage` with option "`-bs 2`" from `.bam` files previously merged with samtools `merge`. Venn diagrams were drawn on R (version 3.4.4; R Core Team 2021) with the package "Vennerable" (version 3.0; Swinton 2013); line plots and heatmaps were plotted using the R packages "gplots" (version 3.0.1; Warnes et al. 2020), "ggplot2" (version 3.1.0; Wickham 2016), "EnrichedHeatmap" (version 1.12.0; Gu et al. 2018) and "wiggleplotr" (version 1.6.1; Alasoo 2020); figures were assembled and further refined in Inkscape (version 0.92.3).

Expression array data analysis

The expression array dataset assessing gene expression in cotyledons isolated from 5-day-old WT Landsberg *erecta* and *35S::CUC1* overexpressing plants re-analyzed in this study was previously published in Takeda et al. (2011). Genes expressed at a low intensity (sum of means of raw intensity < 1) were removed and genes with an absolute fold change > 1.5 in the transformant compared to the control and a *q* value < 0.05 (Benjamini and Hochberg False Discovery Rate) were considered as differentially expressed. Venn diagrams were drawn on R with the package "Vennerable" (version 3.0; Swinton 2013).

RT-qPCR assay

Total RNA was isolated from hypocotyl explants incubated in the specified conditions in triplicates. For each replicate, ~100 hypocotyls were harvested and frozen with liquid nitrogen. The samples were then ground using zirconia ceramic beads in a TissueLyser™ (QIAGEN®) mixer mill. RNA was extracted using the RNeasy® Plant Mini kit (QIAGEN®) following the manufacturer's instructions. The resulting RNA concentrations were determined with a NanoDrop™ 2000 spectrophotometer (Thermo Fisher Scientific®) and normalized between samples. Genomic DNA was removed by incubating the samples for 2 min at 42°C in presence of the gDNA Eraser enzyme (TaKaRa®). Reverse-transcription was then performed using the PrimeScript™ RT reagent Kit (TaKaRa®) following the manufacturer's instructions. Transcript levels were determined with a Mx300P Real-Time PCR System (Agilent®) using the THUNDERBIRD™ SYBR® qPCR Mix (Toyobo®) and the following primers:

- *CUC1*: 5'-`TGCATGAGTATCGCCTTGAC`-3' and 5'-`AACGCCACGCCATCACCGAC`-3' (previously published in Hasson et al. 2011),

- *YUC1*: 5'-TTCCTAAGGGCTGGAGAGGA-3' and 5'-TATTCCTGGTGGACCCCTTC-3',
- *YUC4*: 5'-TAACGAGGAACGGGGCAAAG-3' and 5'-GGCGTTTTTGGCATTCCTTCT-3',
- *PP2AA3*: 5'-TAACGTGGCCAAAATG-3' and 5'-GTTCTCCACAACCGCTTGGT-3'.

Expression values were retrieved from Ct values with an adjustment to each primer pair efficiency, which were determined by dilution series made simultaneously with control WT cDNA. *CUC1*, *YUC1* and *YUC4* expression values were then normalized to *PP2AA3* expression within each sample.

Data Availability

New RNA-seq data generated in this study have been deposited to the Gene Expression Omnibus (GEO) data repository with accession number GSE176161. Raw files from previously published assays which were re-analyzed in this study can be obtained from GEO with accession numbers GSE79355 (for Cortijo et al. (2017)'s dataset), GSE27482 (for Takeda et al. (2011)'s dataset), and GSE134079 (for Zia et al. (2019)'s dataset).

Sequence data for genes investigated in this study can be found in the Arabidopsis Genome Initiative or GenBank/EMBL-EBI databases under the following accession numbers: AT3G15170 (*CUC1*), AT1G76420 (*CUC3*), AT1G24590 (*ESR2*), AT3G12580 (*HSP70*), AT2G38810 (*HTA8*), AT1G52740 (*HTA9*), AT3G54560 (*HTA11*), AT1G68460 (*IPT1*), AT2G37210 (*LOG3*), AT1G13320 (*PP2AA3*), AT4G38850 (*SAUR15*), AT2G17950 (*WUS*), AT4G32540 (*YUC1*) and AT5G11320 (*YUC4*).

Funding

This work was supported by the Special Scholarship for International Students from the University of Tokyo to A.L. and KAKENHI Grants-in-Aid from the Japanese Ministry of Education, Culture, Sports, Science and Technology (MEXT) [19F19781 to D.S.F. and 17H03704, 20H05911 and 20H05905 to K.S.].

Acknowledgments

We are grateful to the members of Cell Function Research Team for discussion and comments on the manuscript.

Author Contributions

A.L., T.T. and K.S. designed research with inputs from B.R., A.I., M.I., S.C., K.E.J. and P.A.W.; A.L., A.K. and T.T. performed regeneration phenotyping assays; A.K. performed RNA-seq experiments, T.S. sequenced RNA-seq libraries and A.L. and T.T. analyzed the data, with inputs from A.I. and M.I.; A.L., D.S.F. and K.S. wrote the manuscript with inputs from all authors.

Disclosures

No conflicts of interest declared.

References

Adams, S., Cockshull, K. E. and Cave, C. R. J. (2001), Effect of Temperature on the Growth and Development

of Tomato Fruits, *Annals of Botany* 88(5):869–877.

Aida, M., Ishida, T., Fukaki, H., Fujisawa, H. and Tasaka, M. (1997), Genes involved in organ separation in *Arabidopsis*: an analysis of the *cup-shaped cotyledon* mutant., *The Plant Cell* 9(6):841–857.

Alasoo, K. (2020), 'wiggleplotr: Make read coverage plots from BigWig files', https://bioconductor.org/packages/release/bioc/html/wiggleplotr.html.

Alexa, A. and Rahnenfuhrer, J. (2020), 'topGO: Enrichment Analysis for Gene Ontology', https://bioconductor.org/packages/release/bioc/html/topGO.html.

Andrews, S. (2010), 'FastQC: A quality control tool for high throughput sequence data', http://www.bioinformatics.babraham.ac.uk/projects/fastqc/.

Auguie, B. (2017), 'gridExtra: Miscellaneous Functions for "Grid" Graphics', https://CRAN.R-project.org/package=gridExtra.

Banno, H., Ikeda, Y., Niu, Q.-W. and Chua, N.-H. (2001), Overexpression of *Arabidopsis ESR1* Induces Initiation of Shoot Regeneration, *The Plant Cell* 13(12):2609–2618.

Benson, E. E. (2000), *In vitro* plant recalcitrance: an introduction, *In Vitro Cellular & Developmental Biology - Plant* 36(3):141-148

Blázquez, M. A., Ahn, J. H. and Weigel, D. (2003), A thermosensory pathway controlling flowering time in *Arabidopsis thaliana*, *Nature Genetics* 33(2):168–171.

Boden, S. A., Kavanová, M., Finnegan, E. J. and Wigge, P. A. (2013), Thermal stress effects on grain yield in *Brachypodium distachyon* occur *via* H2A.Z-nucleosomes, *Genome Biology* 14(6):R65.

Bouyer, D., Roudier, F., Heese, M., Andersen, E. D., Gey, D., Nowack, M. K., Goodrich, J., Renou, J.-P., Grini, P. E., Colot, V. and Schnittger, A. (2011), Polycomb Repressive Complex 2 Controls the Embryo-to-Seedling Phase Transition, *PLoS Genetics* 7(3):e1002014.

Carlson, M. (2020), 'GO.db: A set of annotation maps describing the entire Gene Ontology', https://bioconductor.org/packages/release/data/annotation/html/GO.db.html.

Carter, B., Bishop, B., Ho, K. K., Huang, R., Jia, W., Zhang, H., Pascuzzi, P. E., Deal, R. B. and Ogas, J. (2018), The Chromatin Remodelers PKL and PIE1 Act in an Epigenetic Pathway That Determines H3K27me3 Homeostasis in *Arabidopsis*, *The Plant Cell* 30(6):1337–1352.

Casal, J. J. and Balasubramanian, S. (2019), Thermomorphogenesis, *Annual Review of Plant Biology* 70(1):321–346.

Che, P., Lall, S. and Howell, S. H. (2007), Developmental steps in acquiring competence for shoot development in *Arabidopsis* tissue culture, *Planta* 226(5):1183–1194.

Cheng, Z. J., Wang, L., Sun, W., Zhang, Y., Zhou, C., Su, Y. H., Li, W., Sun, T. T., Zhao, X. Y., Li, X. G., Cheng, Y., Zhao, Y., Xie, Q. and Zhang, X. S. (2012), Pattern of Auxin and Cytokinin Responses for Shoot Meristem Induction Results from the Regulation of Cytokinin Biosynthesis by AUXIN RESPONSE FACTOR3, *Plant Physiology* 161(1):240–251.

Coleman-Derr, D. and Zilberman, D. (2012), Deposition of Histone Variant H2A.Z within Gene Bodies Regulates

Responsive Genes, *PLoS Genetics* 8(10):e1002988.

Cortijo, S., Charoensawan, V., Brestovitsky, A., Buning, R., Ravarani, C., Rhodes, D., van Noort, J., Jaeger, K. E. and Wigge, P. A. (2017), Transcriptional Regulation of the Ambient Temperature Response by H2A.Z Nucleosomes and HSF1 Transcription Factors in *Arabidopsis*, *Molecular Plant* 10(10):1258–1273.

Czechowski, T., Stitt, M., Altmann, T., Udvardi, M. K. and Scheible, W.-R. (2005), Genome-Wide Identification and Testing of Superior Reference Genes for Transcript Normalization in *Arabidopsis*, *Plant Physiology* 139(1):5–17.

Dai, X., Bai, Y., Zhao, L., Dou, X., Liu, Y., Wang, L., Li, Y., Li, W., Hui, Y., Huang, X., Wang, Z. and Qin, Y. (2017), H2A.Z Represses Gene Expression by Modulating Promoter Nucleosome Structure and Enhancer Histone Modifications in *Arabidopsis*, *Molecular Plant* 10(10):1274–1292.

Daimon, Y., Takabe, K. and Tasaka, M. (2003), The *CUP-SHAPED COTYLEDON* Genes Promote Adventitious Shoot Formation on Calli, *Plant and Cell Physiology* 44(2):113–121.

Durinck, S., Moreau, Y., Kasprzyk, A., Davis, S., Moor, B. D., Brazma, A. and Huber, W. (2005), BioMart and Bioconductor: a powerful link between biological databases and microarray data analysis, *Bioinformatics* 21(16):3439–3440.

Durinck, S., Spellman, P. T., Birney, E. and Huber, W. (2009), Mapping identifiers for the integration of genomic datasets with the R/Bioconductor package biomaRt, *Nature Protocols* 4(8):1184–1191.

Feldmann, K. A. and Marks, M. D. (1986), Rapid and efficient regeneration of plants from explants of *Arabidopsis thaliana*, *Plant Science* 47(1):63–69.

Gallois, J.-L. (2004), WUSCHEL induces shoot stem cell activity and developmental plasticity in the root meristem, *Genes & Development* 18(4):375–380.

Gelvin, S. B. (2003), *Agrobacterium*-Mediated Plant Transformation: the Biology behind the “Gene-Jockeying” Tool, *Microbiology and Molecular Biology Reviews* 67(1):16–37.

Gómez-Zambrano, Á., Merini, W. and Calonje, M. (2019), The repressive role of *Arabidopsis* H2A.Z in transcriptional regulation depends on AtBMI1 activity, *Nature Communications* 10(1):2828.

Gordon, S. P., Heisler, M. G., Reddy, G. V., Ohno, C., Das, P. and Meyerowitz, E. M. (2007), Pattern formation during *de novo* assembly of the *Arabidopsis* shoot meristem, *Development* 134(19):3539–3548.

Gray, W. M., Ostin, A., Sandberg, G., Romano, C. P. and Estelle, M. (1998), High temperature promotes auxin-mediated hypocotyl elongation in *Arabidopsis*, *Proceedings of the National Academy of Sciences* 95(12):7197–7202.

Gu, Z., Eils, R., Schlesner, M. and Ishaque, N. (2018), EnrichedHeatmap: an R/Bioconductor package for comprehensive visualization of genomic signal associations, *BMC Genomics* 19(1).

Gyula, P., Baksa, I., Tóth, T., Mohorianu, I., Dalmay, T. and Szittya, G. (2018), Ambient temperature regulates the expression of a small set of sRNAs influencing plant development through NF-YA2 and YUC2, *Plant, Cell & Environment* 41(10):2404–2417.

Haissig, B. E. (1965), Organ formation *in vitro* as applicable to forest tree propagation, *The Botanical Review* 31(4):607–626.

Hasson, A., Plessis, A., Blein, T., Adroher, B., Grigg, S., Tsiantis, M., Boudaoud, A., Damerval, C. and Laufs, P. (2011), Evolution and Diverse Roles of the *CUP-SHAPED COTYLEDON* Genes in *Arabidopsis* Leaf Development, *The Plant Cell* 23(1):54–68.

Hibara, K., Karim, M. R., Takada, S., Taoka, K., Furutani, M., Aida, M. and Tasaka, M. (2006), *Arabidopsis* CUP-SHAPED COTYLEDON3 Regulates Postembryonic Shoot Meristem and Organ Boundary Formation, *The Plant Cell* 18(11):2946–2957.

Howard, B. H. (1971), Propagation Techniques, *Scientific Horticulture* 23(0):116–126.

Ikeda, Y., Banno, H., Niu, Q.-W., Howell, S. H. and Chua, N.-H. (2006), The ENHANCER OF SHOOT REGENERATION 2 gene in *Arabidopsis* Regulates *CUP-SHAPED COTYLEDON 1* at the Transcriptional Level and Controls Cotyledon Development, *Plant and Cell Physiology* 47(11):1443–1456.

Ikeuchi, M., Favero, D. S., Sakamoto, Y., Iwase, A., Coleman, D., Rymen, B. and Sugimoto, K. (2019), Molecular Mechanisms of Plant Regeneration, *Annual Review of Plant Biology* 70(1):377–406.

Ikeuchi, M., Iwase, A., Rymen, B., Lambolez, A., Kojima, M., Takebayashi, Y., Heyman, J., Watanabe, S., Seo, M., De Veylder, L., Sakakibara, H. and Sugimoto, K. (2017), Wounding Triggers Callus Formation *via* Dynamic Hormonal and Transcriptional Changes, *Plant Physiology* 175(3):1158–1174.

Ikeuchi, M., Ogawa, Y., Iwase, A. and Sugimoto, K. (2016), Plant regeneration: cellular origins and molecular mechanisms, *Development* 143(9):1442–1451.

Iwase, A., Harashima, H., Ikeuchi, M., Rymen, B., Ohnuma, M., Komaki, S., Morohashi, K., Kurata, T., Nakata, M., Ohme-Takagi, M., Grotewold, E. and Sugimoto, K. (2017), WIND1 Promotes Shoot Regeneration through Transcriptional Activation of *ENHANCER OF SHOOT REGENERATION1* in *Arabidopsis*, *The Plant Cell* 29(1):54–69.

Iwase, A., Mita, K., Nonaka, S., Ikeuchi, M., Koizuka, C., Ohnuma, M., Ezura, H., Imamura, J. and Sugimoto, K. (2015), WIND1-based acquisition of regeneration competency in *Arabidopsis* and rapeseed, *Journal of Plant Research* 128(3):389–397.

Kakimoto, T. (2001), Identification of Plant Cytokinin Biosynthetic Enzymes as Dimethylallyl Diphosphate: ATP/ADP Isopentenyltransferases, *Plant and Cell Physiology* 42(7):677–685.

Kareem, A., Durgaprasad, K., Sugimoto, K., Du, Y., Pulianmackal, A. J., Trivedi, Z. B., Abhayadev, P. V., Pinon, V., Meyerowitz, E. M., Scheres, B. and Prasad, K. (2015), *PLETHORA* Genes Control Regeneration by a Two-Step Mechanism, *Current Biology* 25(8):1017–1030.

Kim, J.-Y., Yang, W., Forner, J., Lohmann, J. U., Noh, B. and Noh, Y.-S. (2018), Epigenetic reprogramming by histone acetyltransferase HAG1/AtGCN5 is required for pluripotency acquisition in *Arabidopsis*, *The EMBO Journal* 37(20):e98726.

Koini, M. A., Alvey, L., Allen, T., Tilley, C. A., Harberd, N. P., Whitelam, G. C. and Franklin, K. A. (2009), High Temperature-Mediated Adaptations in Plant Architecture Require the bHLH Transcription Factor PIF4, *Current Biology* 19(5):408–413.

Koornneef, M. and Meinke, D. (2010), The development of *Arabidopsis* as a model plant, *The Plant Journal* 61(6):909–21.

Kumar, S. V. and Wigge, P. A. (2010), H2A.Z-Containing Nucleosomes Mediate the Thermosensory Response in *Arabidopsis*, *Cell* 140(1):136–147.

Langmead, B. and Salzberg, S. L. (2012), Fast gapped-read alignment with Bowtie 2, *Nature Methods* 9(4):357–359.

Lardon, R., Wijnker, E., Keurentjes, J. and Geelen, D. (2020), The genetic framework of shoot regeneration in *Arabidopsis* comprises master regulators and conditional fine-tuning factors, *Communications Biology* 3(1):549.

Lee, K. and Seo, P. J. (2017), Coordination of matrix attachment and ATP-dependent chromatin remodeling regulate auxin biosynthesis and *Arabidopsis* hypocotyl elongation, *PLoS One* 12(7):e0181804.

Li, H., Handsaker, B., Wysoker, A., Fennell, T., Ruan, J., Homer, N., Marth, G., Abecasis, G. and Durbin, R. (2009), The Sequence Alignment/Map format and SAMtools, *Bioinformatics* 25(16):2078–2079.

Li, X.-R., Deb, J., Kumar, S. V. and Østergaard, L. (2018), Temperature Modulates Tissue-Specification Program to Control Fruit Dehiscence in Brassicaceae, *Molecular Plant* 11(4):598–606.

Liu, J., Hu, X., Qin, P., Prasad, K., Hu, Y. and Xu, L. (2018), The WOX11-LBD16 pathway promotes pluripotency acquisition in callus cells during *de novo* shoot regeneration in tissue culture, *Plant and Cell Physiology* 59(4):739–748.

Lu, Z., Marand, A. P., Ricci, W. A., Ethridge, C. L., Zhang, X. and Schmitz, R. J. (2019), The prevalence, evolution and chromatin signatures of plant regulatory elements, *Nature Plants* 5(12):1250–1259.

March-Díaz, R. and Reyes, J. C. (2009), The beauty of being a variant: H2a.z and the SWR1 complex in plants, *Molecular Plant* 2(4):565–577.

March-Díaz, R., García-Domínguez, M., Lozano-Juste, J., León, J., Florencio, F. J. and Reyes, J. C. (2007), Histone H2A.Z and homologues of components of the SWR1 complex are required to control immunity in *Arabidopsis*, *The Plant Journal* 53(3):475–487.

Matsuo, N., Makino, M. and Banno, H. (2011), Arabidopsis ENHANCER OF SHOOT REGENERATION (ESR)1 and ESR2 regulate *in vitro* shoot regeneration and their expressions are differentially regulated, *Plant Science* 181(1):39–46.

McCarthy, D. J., Chen, Y. and Smyth, G. K. (2012), Differential expression analysis of multifactor RNA-Seq experiments with respect to biological variation, *Nucleic Acids Research* 40(10):4288–4297.

McKee, M. L., Royer, D. L. and Poulos, H. M. (2019), Experimental evidence for species-dependent responses in leaf shape to temperature: Implications for paleoclimate inference, *PLoS ONE* 14(6):e0218884.

Melnyk, C. W. (2016), Plant grafting: insights into tissue regeneration, *Regeneration* 4(1):3–14.

Meng, W. J., Cheng, Z. J., Sang, Y. L., Zhang, M. M., Rong, X. F., Wang, Z. W., Tang, Y. Y. and Zhang, X. S. (2017), Type-b ARABIDOPSIS RESPONSE REGULATORs specify the shoot stem cell niche by dual regulation of *WUSCHEL*, *The Plant Cell* 29(6):1357–1372.

Motte, H., Vercauteren, A., Depuydt, S., Landschoot, S., Geelen, D., Werbrouck, S., Goormachtig, S., Vuylsteke, M. and Vereecke, D. (2014), Combining linkage and association mapping identifies *RECEPTOR-LIKE PROTEIN KINASE1* as an essential *Arabidopsis* shoot regeneration gene, *Proceedings of the National*

Academy of Sciences 111(22):8305–8310.

Nakayama, H., Nakayama, N., Seiki, S., Kojima, M., Sakakibara, H., Sinha, N. and Kimura, S. (2014), Regulation of the KNOX-GA Gene Module Induces Heterophyllic Alteration in North American Lake Cress, *The Plant Cell* 26(12):4733–4748.

Nikovics, K., Blein, T., Peaucelle, A., Ishida, T., Morin, H., Aida, M. and Laufs, P. (2006), The Balance be- tween the *MIR164A* and *CUC2* Genes Controls Leaf Margin Serration in *Arabidopsis*, *The Plant Cell* 18(11):2929–2945.

Nishimura, T., Hayashi, K., Suzuki, H., Gyohda, A., Takaoka, C., Sakaguchi, Y., Matsumoto, S., Kasahara, H., Sakai, T., Kato, J., Kamiya, Y. and Koshiba, T. (2014), Yucasin is a potent inhibitor of YUCCA, a key enzyme in auxin biosynthesis, *The Plant Journal* 77(3):352–366.

Noh, B., Lee, S.-H., Kim, H.-J., Yi, G., Shin, E.-A., Lee, M., Jung, K.-J., Doyle, M. R., Amasino, R. M. and Noh, Y.-S. (2004), Divergent Roles of a Pair of Homologous Jumonji/Zinc-Finger–Class Transcription Factor Proteins in the Regulation of *Arabidopsis* Flowering Time, *The Plant Cell* 16(10):2601–2613.

Pernisova, M., Grochova, M., Konecny, T., Plackova, L., Harustiakova, D., Kakimoto, T., Heisler, M. G., Novak, O. and Hejatko, J. (2018), Cytokinin signalling regulates organ identity *via* the AHK4 receptor in *Arabidopsis*, *Development* 145(14):dev163907.

Pijut, P. M., Woeste, K. E., Michler, C. H. et al. (2011), Promotion of adventitious root formation of difficult-to-root hardwood tree species, *Horticultural reviews* 38:213.

Quinlan, A. R. and Hall, I. M. (2010), BEDTools: a flexible suite of utilities for comparing genomic features, *Bioinformatics* 26(6):841–842.

R Core Team (2021), 'R: A Language and Environment for Statistical Computing', `https://www.R-project.org/`.

Ramírez, F., Dündar, F., Diehl, S., Grüning, B. A. and Manke, T. (2014), deepTools: a flexible platform for exploring deep-sequencing data, *Nucleic Acids Research* 42(W1):W187–W191.

Robinson, M. D., McCarthy, D. J. and Smyth, G. K. (2009), edgeR: a Bioconductor package for differential expression analysis of digital gene expression data, *Bioinformatics* 26(1):139–140.

Royer, D. L. (2012), Leaf Shape Responds to Temperature but Not CO_2 in *Acer rubrum*, *PLoS ONE* 7(11):e49559.

Rymen, B., Kawamura, A., Lambolez, A., Inagaki, S., Takebayashi, A., Iwase, A., Sakamoto, Y., Sako, K., Favero, D. S., Ikeuchi, M., Suzuki, T., Seki, M., Kakutani, T., Roudier, F. and Sugimoto, K. (2019), Histone acetylation orchestrates wound-induced transcriptional activation and cellular reprogramming in *Arabidopsis*, *Communications Biology* 2(1):404.

Schlenker, W. and Roberts, M. J. (2009), Nonlinear temperature effects indicate severe damages to U.S. crop yields under climate change, *Proceedings of the National Academy of Sciences* 106(37):15594–15598.

Skoog, F. and Miller, C. O. (1957), Chemical regulation of growth and organ formation in plant tissues cultured *in vitro*, *Symposia of the Society for Experimental Biology* 11(1):118–130.

Snipes, S. A., Rodriguez, K., DeVries, A. E., Miyawaki, K. N., Perales, M., Xie, M. and Reddy, G. V. (2018),

Cytokinin stabilizes WUSCHEL by acting on the protein domains required for nuclear enrichment and transcription, *PLoS Genetics* 14(4):e1007351.

Sugimoto, K., Jiao, Y. and Meyerowitz, E. M. (2010), *Arabidopsis* Regeneration from Multiple Tissues Occurs via a Root Development Pathway, *Developmental Cell* 18(3):463–471.

Sun, J., Qi, L., Li, Y., Chu, J. and Li, C. (2012), PIF4–Mediated Activation of *YUCCA8* Expression Integrates Temperature into the Auxin Pathway in Regulating *Arabidopsis* Hypocotyl Growth, *PLoS Genetics* 8(3):e1002594.

Sura, W., Kabza, M., Karlowski, W. M., Bieluszewski, T., Kus-Slowinska, M., Pawełoszek, Ł., Sadowski, J. and Ziolkowski, P. A. (2017), Dual Role of the Histone Variant H2A.Z in Transcriptional Regulation of Stress-Response Genes, *The Plant Cell* 29(4):791–807.

Swinton, J. (2013), 'Vennerable: Venn and Euler area-proportional diagrams', https://R-Forge.R-project. org/projects/vennerable/.

Takeda, S., Hanano, K., Kariya, A., Shimizu, S., Zhao, L., Matsui, M., Tasaka, M. and Aida, M. (2011), CUP-SHAPED COTYLEDON1 transcription factor activates the expression of *LSH4* and *LSH3*, two members of the ALOG gene family, in shoot organ boundary cells, *The Plant Journal* 66(6):1066–1077.

Takei, K., Sakakibara, H. and Sugiyama, T. (2001), Identification of Genes Encoding Adenylate Isopentenyltransferase, a Cytokinin Biosynthesis Enzyme, in *Arabidopsis thaliana*, *Journal of Biological Chemistry* 276(28):26405–26410.

Tasset, C., Yadav, A. S., Sureshkumar, S., Singh, R., van der Woude, L., Nekrasov, M., Tremethick, D., van Zanten, M. and Balasubramanian, S. (2018), POWERDRESS-mediated histone deacetylation is essential for thermomorphogenesis in *Arabidopsis thaliana*, *PLoS Genetics* 14(3):e1007280.

Thakar, A., Gupta, P., McAllister, W. T. and Zlatanova, J. (2010), Histone Variant H2A.Z Inhibits Transcription in Reconstituted Nucleosomes, *Biochemistry* 49(19):4018–4026.

Thatcher, T. H. and Gorovsky, M. A. (1994), Phylogenetic analysis of the core histones H2A, H2B, H3, and H4, *Nucleic Acids Research* 22(2):174–179.

Valvekens, D., Montagu, M. V. and Lijsebettens, M. V. (1988), *Agrobacterium tumefaciens*-mediated transformation of *Arabidopsis thaliana* root explants by using kanamycin selection, *Proceedings of the National Academy of Sciences* 85(15):5536–5540.

van der Woude, L. C., Perrella, G., Snoek, B. L., van Hoogdalem, M., Novák, O., van Verk, M. C., van Kooten, H. N., Zorn, L. E., Tonckens, R., Dongus, J. A., Praat, M., Stouten, E. A., Proveniers, M. C. G., Vel- lutini, E., Patitaki, E., Shapulatov, U., Kohlen, W., Balasubramanian, S., Ljung, K., van der Krol, A. R., Smeekens, S., Kaiserli, E. and van Zanten, M. (2019), HISTONE DEACETYLASE 9 stimulates auxin-dependent thermomorphogenesis in *Arabidopsis thaliana* by mediating H2A.Z depletion, *Proceedings of the National Academy of Sciences* 116(50):25343–25354.

Vuylsteke, D. and Swennen, R. (1992), Genetic improvement of plantains: the potential of conventional approaches and the interface with *in-vitro* culture and biotechnology, *in* 'Proceedings of the workshop on Biotechnology Applications for Banana and Plantain Improvement. San José, Costa Rica', Vol. 2731, pp. 169–176.

Wang, E. et al. (2017), The uncertainty of crop yield projections is reduced by improved temperature response functions, Nature Plants 3(8):17102.

Warnes, G. R., Bolker, B., Bonebakker, L., Gentleman, R., Huber, W., Liaw, A., Lumley, T., Maechler, M., Magnusson, A., Moeller, S., Schwartz, M. and Venables, B. (2020), 'gplots: Various R Programming Tools for Plotting Data', https://CRAN.R-project.org/package=gplots.

Weckx, S., Inzé, D. and Maene, L. (2019), Tissue Culture of Oil Palm: Finding the Balance Between Mass Propagation and Somaclonal Variation, *Frontiers in Plant Science* 10(8):722.

Wickham, H. (2016), *ggplot2: Elegant Graphics for Data Analysis*, Springer-Verlag New York.

Wilke, C. O. (2020), 'cowplot: Streamlined Plot Theme and Plot Annotations for 'ggplot2", https://CRAN. R-project.org/package=cowplot.

Willige, B. C., Zander, M., Yoo, C. Y., Phan, A., Garza, R. M., Trigg, S. A., He, Y., Nery, J. R., Chen, H., Chen, M., Ecker, J. R. and Chory, J. (2021), PHYTOCHROME-INTERACTING FACTORs trigger environmentally responsive chromatin dynamics in plants, *Nature Genetics* 53(8):955–961.

Xu, M., Leichty, A. R., Hu, T. and Poethig, R. S. (2017), H2A.Z promotes the transcription of *MIR156A* and *MIR156C* in *Arabidopsis* by facilitating the deposition of H3K4me3, *Development* 145(2):dev152868.

Xu, S., Grullon, S., Ge, K. and Peng, W. (2014), Spatial Clustering for Identification of ChIP-Enriched Regions (SICER) to map regions of histone methylation patterns in embryonic stem cells, *in* 'Methods in Molecular Biology', Springer New York, pp. 97–111.

Xue, M., Zhang, H., Zhao, F., Zhao, T., Li, H. and Jiang, D. (2021), The INO80 chromatin remodeling complex promotes thermomorphogenesis by connecting H2A.Z eviction and active transcription in *Arabidopsis*, *Molecular Plant* 14(11):1799–1813.

Yu, G. (2020), 'ggplotify: Convert Plot to 'grob' or 'ggplot' Object', https://CRAN.R-project.org/package= ggplotify.

Zander, M., Willige, B. C., He, Y., Nguyen, T. A., Langford, A. E., Nehring, R., Howell, E., McGrath, R., Bartlett, A., Castanon, R., Nery, J. R., Chen, H., Zhang, Z., Jupe, F., Stepanova, A., Schmitz, R. J., Lewsey, M. G., Chory, J. and Ecker, J. R. (2019), Epigenetic silencing of a multifunctional plant stress regulator, *eLife* 8.

Zhai, N. and Xu, L. (2021), Pluripotency acquisition in the middle cell layer of callus is required for organ regeneration, *Nature Plants* 7(11):1453–1460.

Zheng, S., Hu, H., Ren, H., Yang, Z., Qiu, Q., Qi, W., Liu, X., Chen, X., Cui, X., Li, S., Zhou, B., Sun, D., Cao, X. and Du, J. (2019), The *Arabidopsis* H3K27me3 demethylase JUMONJI 13 is a temperature and photoperiod dependent flowering repressor, *Nature Communications* 10(1):1303.

Zia, S. F., Berkowitz, O., Bedon, F., Whelan, J., Franks, A. E. and Plummer, K. M. (2019), Direct comparison of *Arabidopsis* gene expression reveals different responses to melatonin *versus* auxin, *BMC Plant Biology* 19(1):567.

Zilberman, D., Coleman-Derr, D., Ballinger, T. and Henikoff, S. (2008), Histone H2A.Z and DNA methylation are mutually antagonistic chromatin marks, *Nature* 456(7218):125–129.

Legends to Figures

Figure 1: Hormone-induced regeneration efficiency increases at warmer temperatures.

(A) Light microscopy images of WT hypocotyl explants incubated on CIM for 4, 15 or 25 days at 17°C, 22°C or 27°C. Scale bars = 5 mm.

(B) Fresh weight of WT hypocotyl explants incubated on CIM for 4, 15 or 25 days at 17°C, 22°C or 27°C (n ≥ 17). Values were normalized to the post-cutting length of explants. **p* value < 0.05. ***p* value < 0.01. ****p* value < 0.001 (Student's *t*-test).

(C) Light microscopy images of WT hypocotyl explants incubated on CIM for 4 days and then on SIM for 4, 11 or 21 days at 17°C, 22°C or 27°C. White arrows indicate flower buds. Scale bars = 5 mm.

(D) Number of shoots produced per WT hypocotyl explant after incubation on CIM for 4 days and then on SIM for 4, 11 or 21 days at 17°C, 22°C or 27°C (n ≥ 3). **p* value < 0.05. ***p* value < 0.01. ****p* value < 0.001 (Student's *t*-test).

Figure 2: Numerous regeneration genes are transcriptionally affected by warm temperature during hormone-induced regeneration.

(A) Venn diagram representation of the overlap between CIM-induced genes, SIM-induced genes and thermo-induced genes. CIM-induced genes include those induced after CIM incubation at either 17°C or 27°C compared to right after cutting. SIM-induced genes include those induced after CIM+SIM incubation at either 17°C or 27°C compared to right after cutting. Thermo-induced genes include those up-regulated at 27°C compared to 17°C either after CIM or after CIM+SIM incubation. The enrichment (representation factor, hypergeometric test) of genes up-regulated at 27°C among all genes up-regulated by CIM or CIM+SIM incubation is indicated. ****p* value < 0.001.

(B) Top 10 GO terms enriched among genes induced by CIM and/or SIM and up-regulated at 27°C.

(C) Line graphs showing the expression of *IPT1*, *LOG3*, *CUC1*, *CUC3*, *ESR2*, *WUS*, *YUC1*, *YUC4* and *SAUR15*. Explants were incubated on CIM for 4 days and then on SIM for 4 days at 17°C or 27°C. *HSP70* is shown as a reference temperature-induced gene (Kumar and Wigge 2010) and *PROTEIN PHOSPHATASE 2A SUBUNIT A3* (*PP2AA3*) as a reference non-induced gene (Czechowski et al. 2005). Error bars show the standard deviation between three sequencing replicates. **p* value < 0.05. ***p* value < 0.01. ****p* value < 0.001 (Student's *t*-test, n = 3).

Figure 3: Differential regulation of gene expression at 27°C correlates with changes in H2A.Z enrichment.

(A) Venn diagram representation of the overlap between thermo- and CIM/SIM-induced genes and genes with temperature-dependent HTA11 enrichment. Thermo- and CIM/SIM-induced genes include CIM- and/or SIM-induced genes that are up-regulated at 27°C compared to 17°C on either medium. Genes with temperature-dependent HTA11 enrichment include those that lose or gain HTA11 within the chromatin spanning their coding region plus 2 upstream nucleosomes (294 bp) in plants transferred to 27°C compared to plants maintained at 17°C. The enrichment (representation factor, hypergeometric test) of thermo- and CIM/SIM-induced genes among genes with temperature-dependent HTA11 enrichment is indicated. ***p* value < 0.01. ****p* value < 0.001.

(B) Heat map representation of the normalized ChIP-seq read density distribution for HTA11 within the chromatin spanning the coding region plus 2 upstream nucleosomes (294 bp) of all HTA11-marked genes in plants transferred to 27°C or plants maintained at 17°C. The position of the transcription start site (TSS) and

transcription termination site (TTS) is marked. Line graphs show the summed HTA11 enrichment for HTA11-marked genes that are thermo- induced and up-regulated on CIM/SIM, HTA11-marked genes that are thermo-repressed and down-regulated on CIM/SIM and all other HTA11-marked genes. For the sake of clarity, only a subset of randomly chosen other HTA11-marked genes is shown in the heat maps, but the whole group is taken into account in the line graphs.

(C) Line plots showing the HTA11 occupancy across the coding region of *IPT1*, *LOG3*, *CUC1*, *CUC3*, *ESR2*, *WUS*, *YUC1*, *YUC4* and *SAUR15*. Data are shown for 240 min at 17°C or after transfer to 27°C. *HSP70* is shown as a reference temperature-induced gene (Kumar and Wigge 2010) and *PP2AA3* as a reference non-induced gene (Czechowski et al. 2005).

Figure 4: The enhancement of shoot regeneration in h2a.z *mutants is stronger at cooler temperatures than at warmer temperatures.*

(A) Light microscopy images of WT, *hta9-1;hta11-1* and *hta9-1;hta11-2* hypocotyl explants incubated on CIM for 4 days and then on SIM for 11 days at 17°C, 22°C or 27°C. Scale bars = 10 mm.

(B) Number of shoots produced per WT, *hta9-1;hta11-1* and *hta9-1;hta11-2* hypocotyl explant after incubation on CIM for 4 days and then on SIM for 11 days at 17°C, 22°C or 27°C (n ≥ 8). **p* value < 0.05. ***p* value < 0.01 (Student's *t*-test).

(C) Light microscopy images of WT, *hta9-1;hta11-1* and *hta9-1;hta11-2* hypocotyl explants incubated on CIM for 4 days and then on SIM for 16 days at 17°C, 22°C or 27°C. Scale bars = 10 mm.

(D) Number of shoots produced per WT, *hta9-1;hta11-1* and *hta9-1;hta11-2* hypocotyl explant after incubation on CIM for 4 days and then on SIM for 16 days at 17°C, 22°C or 27°C (n = 9). **p* value < 0.05. ***p* value < 0.01 (Student's *t*-test).

(E) Light microscopy images of WT, *hta9-1;hta11-1* and *hta9-1;hta11-2* hypocotyl explants incubated on CIM for 4 days and then on SIM for 29 days at 17°C. Scale bars = 10 mm.

(F) Number of shoots produced per WT, *hta9-1;hta11-1* and *hta9-1;hta11-2* hypocotyl explant after incubation on CIM for 4 days and then on SIM for 29 days at 17°C (n = 9). ***p* value < 0.01 (Student's *t*-test).

Figure 5: A mutation in CUC1 *impairs the enhancement of regeneration by warm temperature.*

(A) RT-qPCR analysis showing the expression of *CUC1* in WT and *hta9-1;hta11-1* hypocotyl explants incubated on CIM for 4 days then on SIM for 4 days at 17°C or 27°C. Gene expression levels were normalized to *PP2AA3* expression. Error bars show the standard deviation between three biological replicates. **p* value < 0.05. ***p* value < 0.01 (Student's *t*-test, n = 3).

(B) Venn diagram representation of the overlaps between thermo-induced genes and CUC1-induced genes. Thermo-induced genes include those up-regulated at 27°C compared to 17°C on either CIM or SIM. CUC1-induced genes include those up-regulated in 5-day-old cotyledons from *35S::CUC1* overexpressors compared to the WT (Landsberg *erecta*; data from Takeda et al. (2011)). The enrichment (representation factor, hypergeometric test) between thermo-induced genes and CUC1-induced genes is indicated. ****p* value < 0.001.

(C) Light microscopy images of WT and *cuc1-13* hypocotyl explants incubated on CIM for 4 days and then on SIM for 11 days, at either 17°C or 27°C. Scale bars = 5 mm.

(D) Number of shoots produced per WT and *cuc1-13* hypocotyl explant after incubation on CIM for 4 days and then on SIM for 11 days at 17°C or 27°C (n ≥ 15). ****p* value < 0.001 (Student's *t*-test).

Figure 6: Increased YUC4 *expression is partially responsible for enhanced hormone-induced regeneration at warmer temperatures.*

(A) RT-qPCR analysis showing the expression of *YUC1* and *YUC4* in WT and *hta9-1;hta11-1* hypocotyl explants incubated on CIM for 4 days then on SIM for 4 days at 17°C or 27°C. Gene expression levels were normalized to *PP2AA3* expression. Error bars show the standard deviation between three biological replicates. **p* value < 0.05. ***p* value < 0.01 (Student's *t*-test, n = 3).

(B) Venn diagram representation of the overlaps between thermo-induced genes and auxin-induced genes. Thermo-induced genes include those up-regulated at 27°C compared to 17°C on either CIM or SIM. Auxin-induced genes include those up-regulated in 15-day-old rosettes from seedlings incubated for 3 days on regular medium supplemented with 4.5 µM auxin (NAA; data from Zia et al. (2019)). The enrichment (representation factor, hypergeometric test) between thermo-induced genes and auxin-induced genes is indicated. ****p* value < 0.001.

(C) Light microscopy images of WT hypocotyl explants incubated at 17°C or 27°C for 4 days on CIM and then for 11 days on SIM. CIM and SIM were supplemented with DMSO or 10 µM yucasin (yuc). Scale bars = 5 mm.

(D) Number of shoots produced per WT hypocotyl explant after incubation at either 17°C or 27°C for 4 days on CIM and then for 11 days on SIM. CIM and SIM were supplemented with DMSO or 10 µM yucasin (yuc; n ≥ 6). **p* value < 0.05. ***p* value < 0.01 (Student's *t*-test).

Figure 1

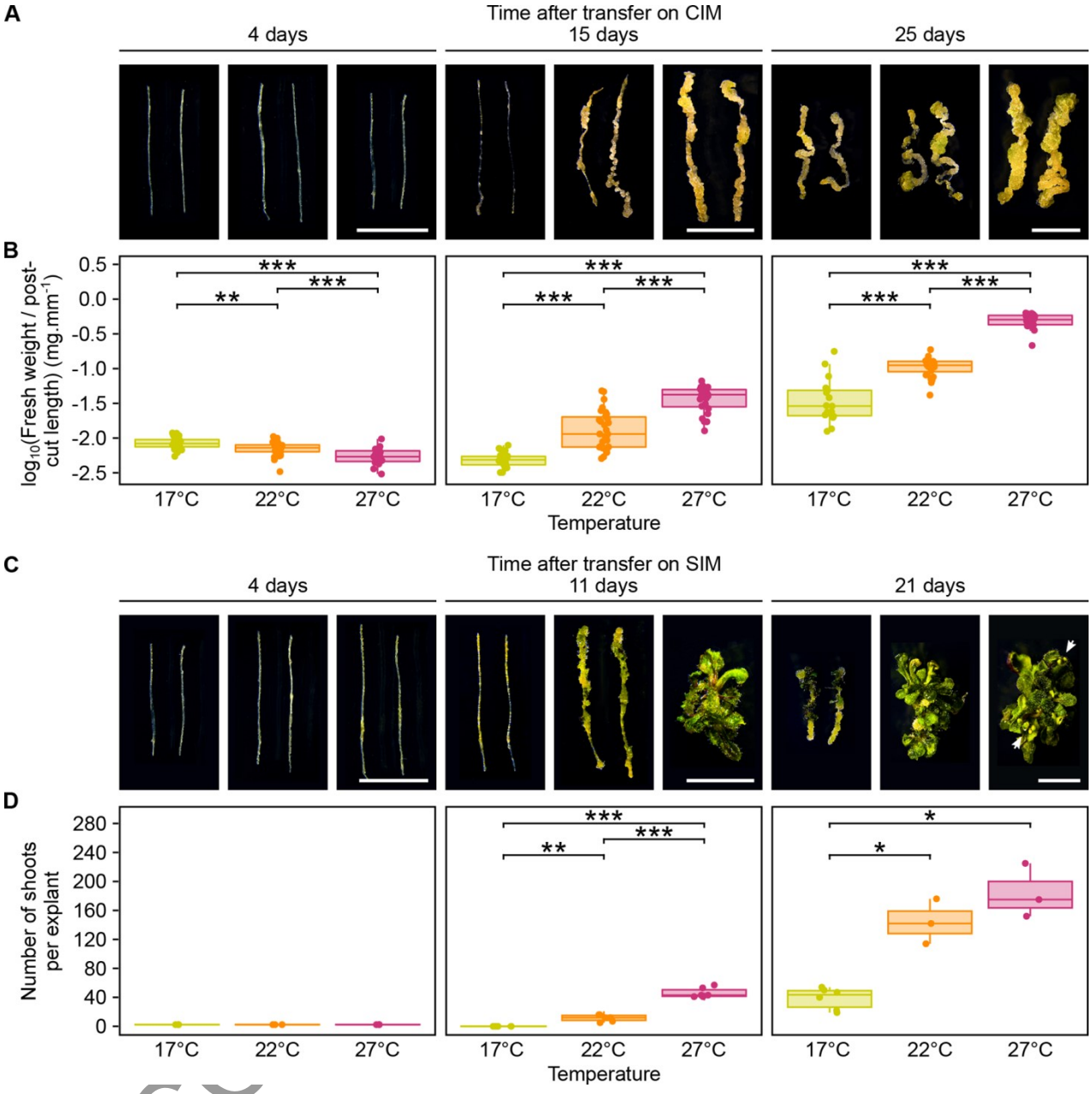

Figure 2

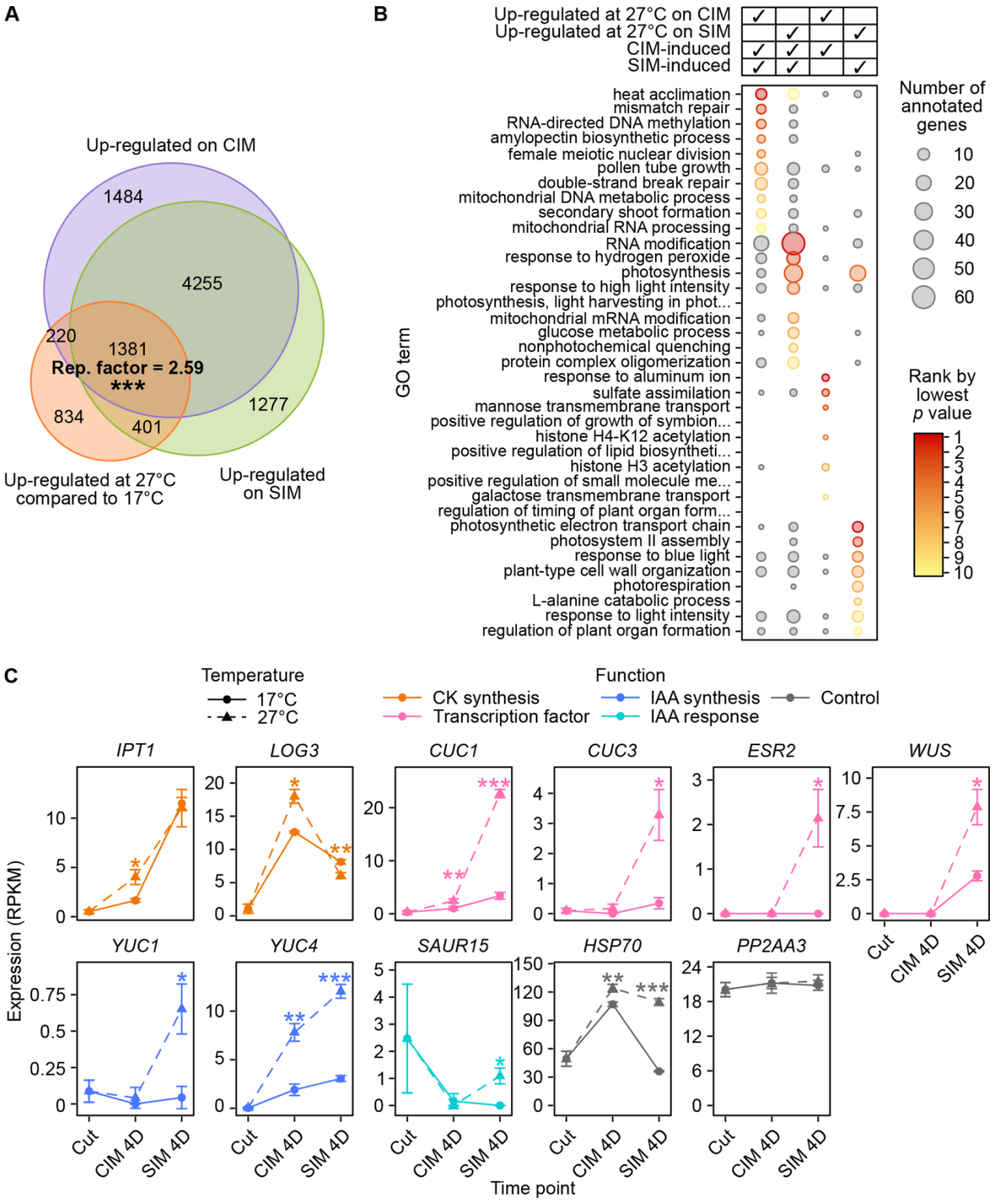

Figure 3

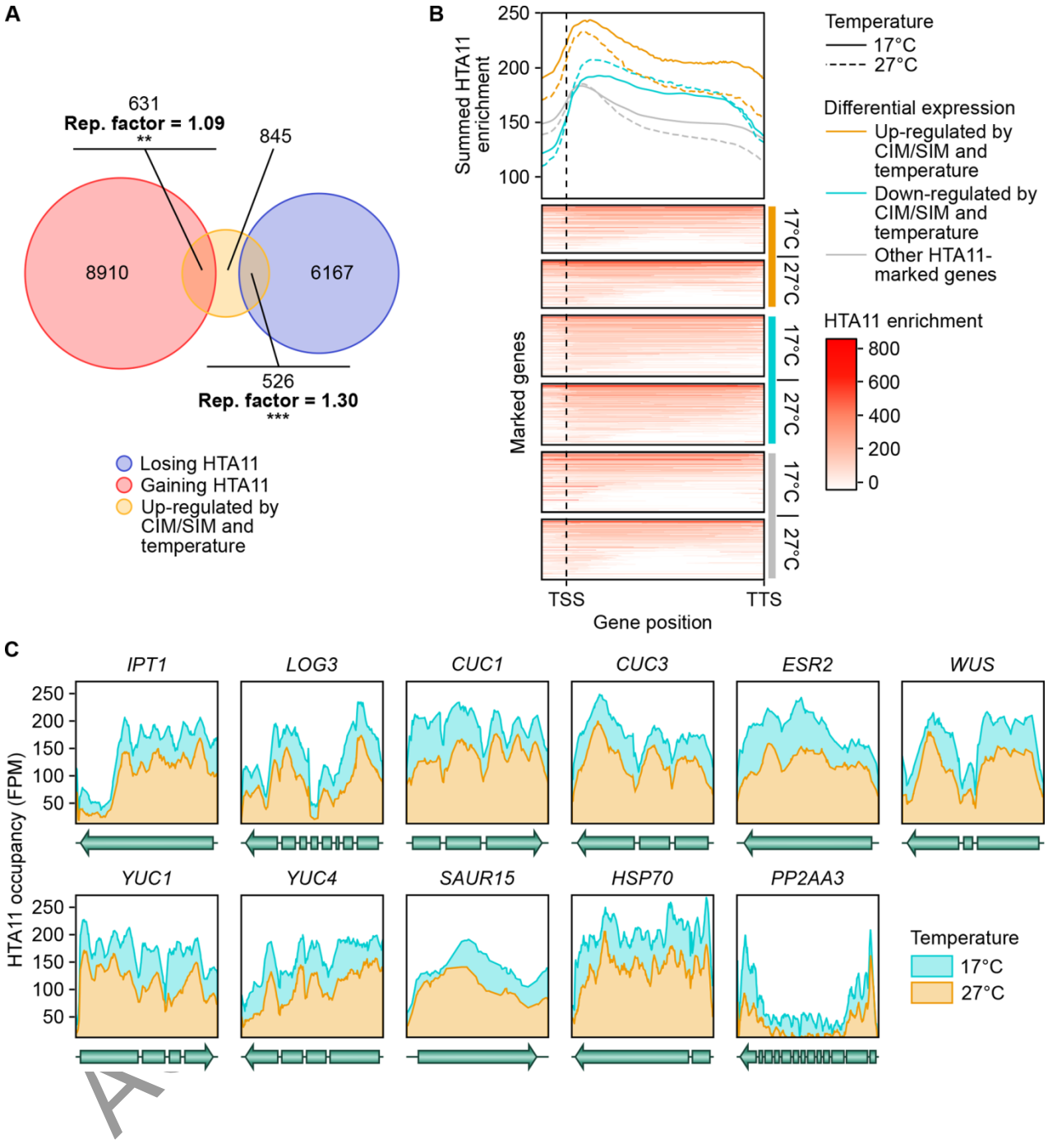

Figure 4

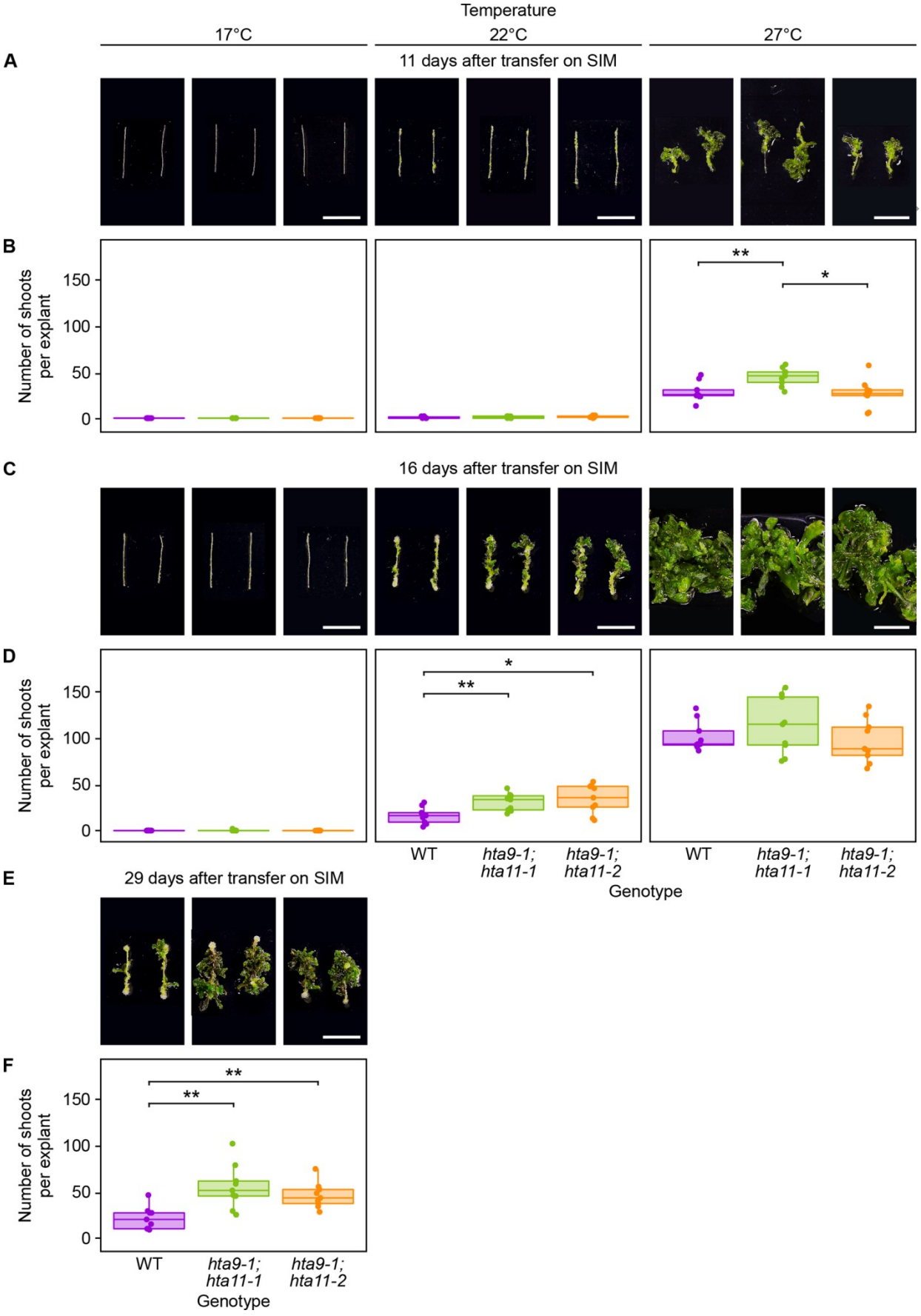

Figure 5

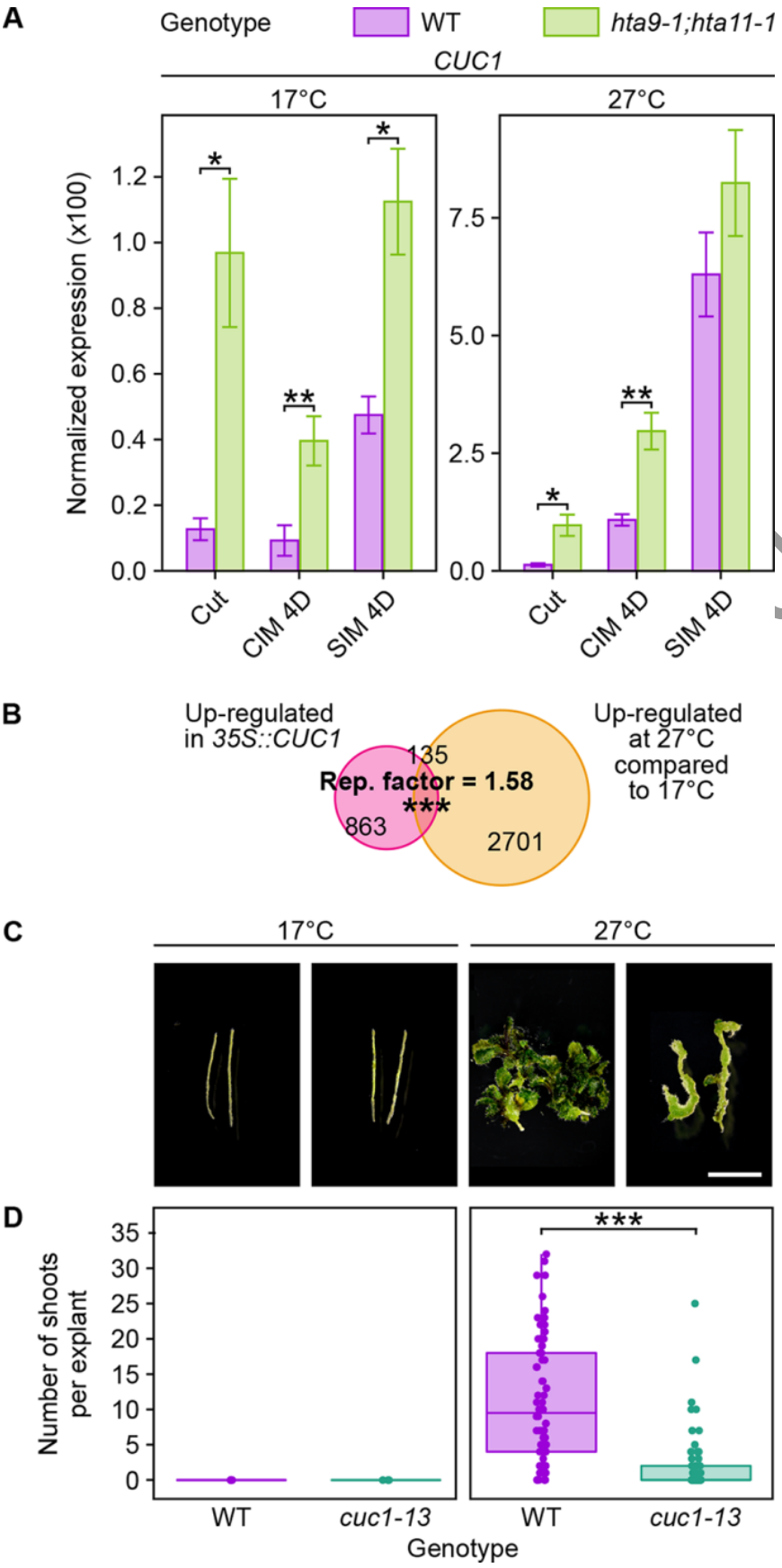

Figure 6